Precambrian Research 175 (2009) 116–134

Contents lists available at ScienceDirect

Precambrian Research

journal homepage: www.elsevier.com/locate/precamres

Geochemistry and tectonic evolution of the Neoproterozoic incipient arc–forearc crust in the Fawakhir area, Central Eastern Desert of Egypt

Yasser Abd El-Rahman[a,d,*], Ali Polat[a], Yildrim Dilek[b], Brian J. Fryer[a,c], Mohamed El-Sharkawy[d], Shawki Sakran[d]

[a] Department of Earth and Environmental Sciences, University of Windsor, Windsor, ON, Canada N9B 3P4
[b] Department of Geology, Miami University, Oxford, OH 45056, USA
[c] Great Lake Institute for Environmental Research, University of Windsor, ON, Canada N9B 3P4
[d] Geology Department, Cairo University, Giza 12613, Egypt

ARTICLE INFO

Article history:
Received 9 March 2009
Received in revised form
15 September 2009
Accepted 20 September 2009

Keywords:
Subduction initiation
Ophiolite
Active continental margin
Neoproterozoic
Arabian-Nubian Shield
Egypt

ABSTRACT

The geodynamic origin of the Neoproterozoic ophiolites of the Arabian-Nubian Shield exposed in the Eastern Desert of Egypt remains controversial. In this study, we present new geochemical and field data from the Fawakhir ophiolite and from some mélange blocks along the Qift-Qusier Road in order to constraint the tectonic evolution of this part of the Central Eastern Desert. The Fawakhir ophiolite contains most lithological units of a Penrose-type ophiolite sequence, and includes ultramafic rocks in the west overlain by isotropic gabbro, sheeted dikes and pillow basalt in the east. These ophiolitic units are enriched in LREE (light rare earth elements) and LILE (large ion lithophile elements) but depleted in high field strength elements (La/Sm_{cn} = 0.40–1.22, Th/Nb_{pm} = 1.7–10.9, La/Nb_{pm} = 1.4–6.6). Their magmas appear to have been derived from a depleted (N-MORB-like) mantle source, and their geochemical characteristics are comparable to those of the Izu-Bonin-Mariana forearc oceanic crust formed during the initiation of an intra-oceanic subduction zone. Pillow lava blocks in the eastern mélange have geochemical signatures similar to those of oceanic crust generated in back-arc basins. The decrease in the magnitude of mantle depletion and the change of the geochemical signature along the Qift-Qusier Road from a forearc in the west to a back-arc in the east suggest the formation of the Fawakhir intra-oceanic arc system over an east-dipping subduction zone. With continued subduction and arc migration, this intra-oceanic arc system finally collided with the passive margin of the West Gondwana (the Saharan craton), resulting in the accretion of the Fawakhir arc–forearc units. Following its tectonic accretion onto the West Gondwana continental margin, the Fawakhir ophiolite was intruded by calc-alkaline dikes, whose magmas were derived partly from partial melting of the sub-continental lithospheric mantle. These dikes have geochemical characteristics similar to those of modern active continental margin (Andean-type) rocks (La/Sm_{cn} = 2.13–2.48, Gd/Yb_{cn} = 2.04–4.25, Th/Nb_{pm} = 3.2–5.8, La/Nb_{pm} = 2.5–4.9), suggesting that the West Gondwana passive margin (Atlantic-type) was converted to an Andean-type margin subsequent to the arc-continent collision. The inferred conversion of the Atlantic-type margin to an Andean-type margin resulted from the collision-induced reversal of the subduction direction.

1. Introduction

The Neoproterozoic Era is characterized by the widespread formation of ophiolites (Stern, 2005, 2008), which are particularly common in the Arabian-Nubian Shield with ages ranging from 870 to 690 Ma (Dilek and Ahmed, 2003; Stern et al., 2004). Neoproterozoic crustal growth of the Arabian-Nubian Shield was accomplished mostly through the accretion of island arcs to continental margins, as the Mozambique Ocean between the West and East Gondwana supercontinents was closed (Furnes et al., 1996; El-Shafei and Kusky, 2003; Jöns and Schenk, 2007, and references therein). The final collision between West and East Gondwana resulted in the Pan-African orogeny (Kröner, 1985; Kröner et al., 1987). Subduction, accretion, and crustal thickening processes took place between about 870 and 570 Ma (Stern and Hedge, 1985; Kröner et al., 1992; Stern, 1994). The crustal evolution of the Eastern Desert culminated in the eruption of the Dokhan Volcanics, deposition of molasse-type Hammamat sediments, and emplacement of younger granites (Eliwa et al., 2006).

* Corresponding author at: Geology Department-Faculty of Science, Cairo University, Giza 12613, Egypt.
E-mail addresses: yasser@uwindsor.ca, yassermedhat@hotmail.com (Y. Abd El-Rahman).

0301-9268/$ – see front matter © 2009 Elsevier B.V. All rights reserved.
doi:10.1016/j.precamres.2009.09.008

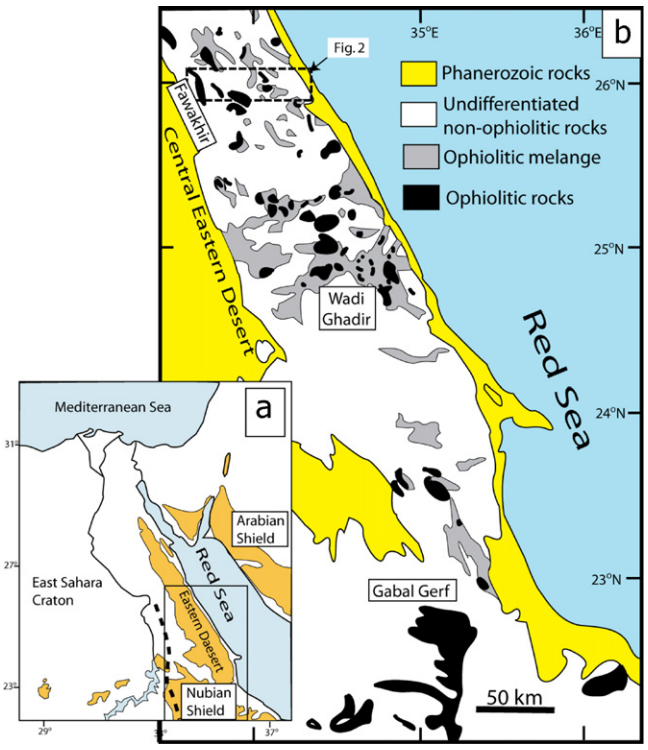

Fig. 1. (a) Distribution of Precambrian basement exposures on both sides of the Red Sea. The dashed line is the approximate boundary between the Shield and the Eastern Saharan Craton (after Greiling et al., 1994). (b) Distribution of ophiolitic fragments in the Eastern Desert of Egypt. Modified from El-Sayed et al. (1999).

The Eastern Desert of Egypt constitutes the northwestern end of the Nubian segment of the Arabian-Nubian Shield (Fig. 1a). Despite recent progress in understanding the evolution of the Arabian-Nubian Shield, the tectonic setting of the ophiolites in the Eastern Desert still remains unresolved. As for many other ophiolites, the ophiolitic rocks of the Arabian-Nubian Shield have supra-subduction geochemical signatures (Stern et al., 2004), but Zimmer et al. (1995) reported the occurrence of mid-ocean ridge (MOR) ophiolite in the Gerf area in the southern Eastern Desert (Fig. 1b). The supra-subduction signature of the ophiolites in the Eastern Desert led to further debate on whether they were formed in a back-arc setting (El-Bayoumi, 1983; Furnes et al., 1996; El-Sayed et al., 1999; Farahat et al., 2004) or in a forearc setting during subduction initiation (Azer and Stern, 2007; Khalil and Azer, 2007).

Azer and Stern (2007) and Khalil and Azer (2007) proposed that the Neoproterozoic ophiolites of the Eastern Desert were formed in a forearc setting based on the depleted nature of the serpentinized mantle rocks. Although their conclusion is consistent with other Arabian-Nubian Shield ophiolitic mantle units (Stern et al., 2004), alternative geodynamic settings have been proposed for the upper-mantle peridotites of the Central Eastern Desert. For example, Ahmed et al. (2001) and Farahat (2008) suggested that harzburgites are likely to be fragments of back-arc basin lithosphere. Khalil (2007) inferred a mid-ocean ridge tectonic setting for the mantle rocks of Wadi Ghadir ophiolite in the Eastern Desert. Ophiolitic gabbros and pillow lavas in the Central Eastern Desert were interpreted as remnants of oceanic crust formed in a back-arc basin (Kröner, 1985; El-Sayed et al., 1999; Farahat et al., 2004; Abd El-Naby and Frisch, 2006).

In this study, new major element (40 samples) and trace element (58 samples) data obtained from different crustal units of the Fawakhir ophiolite along with some samples from the mélange along Qift-Qusier Road and the younger dikes crosscutting the ophiolitic units are reported. These geochemical data and field observations are used in order to: (1) evaluate the tectonic setting of the formation of the Fawakhir ophiolite; (2) decipher the mantle melt source of its crustal units; and (3) re-evaluate the existing geodynamic models to better constrain the changes in subduction direction associated with the documented incipient arc generation and post-accretion magmatism.

2. Previous work on the Fawakhir ophiolite

Shackleton et al. (1980) identified the mafic–ultramafic rocks along the Qift-Qusier Road in the Central Eastern Desert, including the Fawakhir area, as an ophiolitic assemblage (Fig. 2). Nasseef et al. (1980) defined the whole ophiolitic sequence, starting from the ultramafic rocks at the base through gabbroic rocks and sheeted dikes to the basic pillow lavas at the top (Fig. 3). Using geochemistry, Stern (1981) divided the Neoproterozoic volcanic rocks in the Central Eastern Desert into an older (Older Metavolcanics) and a younger (Younger Metavolcanics) volcanic assemblage. The older assemblage is interpreted as a remnant of oceanic crust, whereas the younger assemblage is interpreted as an island arc sequence. Stern (1981) considered the Fawakhir mafic rocks as part of the older assemblage formed in either small oceanic rift or back-arc basin. In their geodynamic model for the evolution of the Central Eastern Desert, Ries et al. (1983) considered the Fawakhir ophiolite as a mid-ocean-generated oceanic crust that has been preserved in an olistostromal mélange. El-Gaby et al. (1988) considered the Fawakhir ophiolite as a segment of oceanic crust formed in a marginal (back-arc?) basin, similar to the Wadi Ghadir ophiolite farther south.

El-Sayed et al. (1999) reported the most comprehensive geochemical data on the Fawakhir ophiolite. They stated that the Fawakhir ophiolite is composed of tholeiitic to calc-alkaline gabbros and volcanic rocks, and also includes minor boninitic gabbros. From the association of arc-type lava, plume-type MORB and boninitic rocks, El-Sayed et al. (1999) proposed that the Fawakhir ophiolite was formed in back-arc basin. Andresen et al. (2009) implied that the Fawakhir ophiolite possibly formed in a forearc setting.

3. Regional geology and field characteristics

Qift-Qusier Road traverses the Neoproterozoic basement rocks of the Central Eastern Desert (CED). The NW-SE-trending Precambrian rocks along this road are unconformably overlain by the Cretaceous Nubian sandstone to the west and by Miocene siliciclastic sedimentary rocks to the east and can be grouped into three units: (1) the Meatiq quartzofeldspathic gneisses, (2) the ophiolitic mélange, and (3) the Hamammat molasse-type siliciclastic sedimentary rocks (El-Gaby et al., 1984) (Fig. 2). All these units are tectonically juxtaposed. The mélange is composed of dismembered ophiolitic fragments (serpentinized peridotite, pyroxenite, gabbros, and volcanic rocks), island arc-related andesitic volcanic and volcaniclastic rocks, and amphibolite dispersed in a sheared sedimentary matrix (Ries et al., 1983; El-Gaby et al., 1984; Fowler and Osman, 2001).

Ophiolitic units of the CED occur as dismembered blocks in a tectonic mélange (Shackleton et al., 1980; Ries et al., 1983; El-Gaby et al., 1988) (Fig. 1b). The best exposures of the ophiolitic units along the Qift-Qusier Road occur in the Fawakhir area, which is located between the Meatiq gneissic dome to the east and the Hamammat sedimentary rocks to the west (Nasseef et al., 1980). The Fawakhir ophiolitic sequence includes, from the bottom to the top, ultramafic rocks, gabbros and volcanic rocks, mainly basalt and basaltic andesite towards the east (El-Sayed et al., 1999) (Fig. 3).

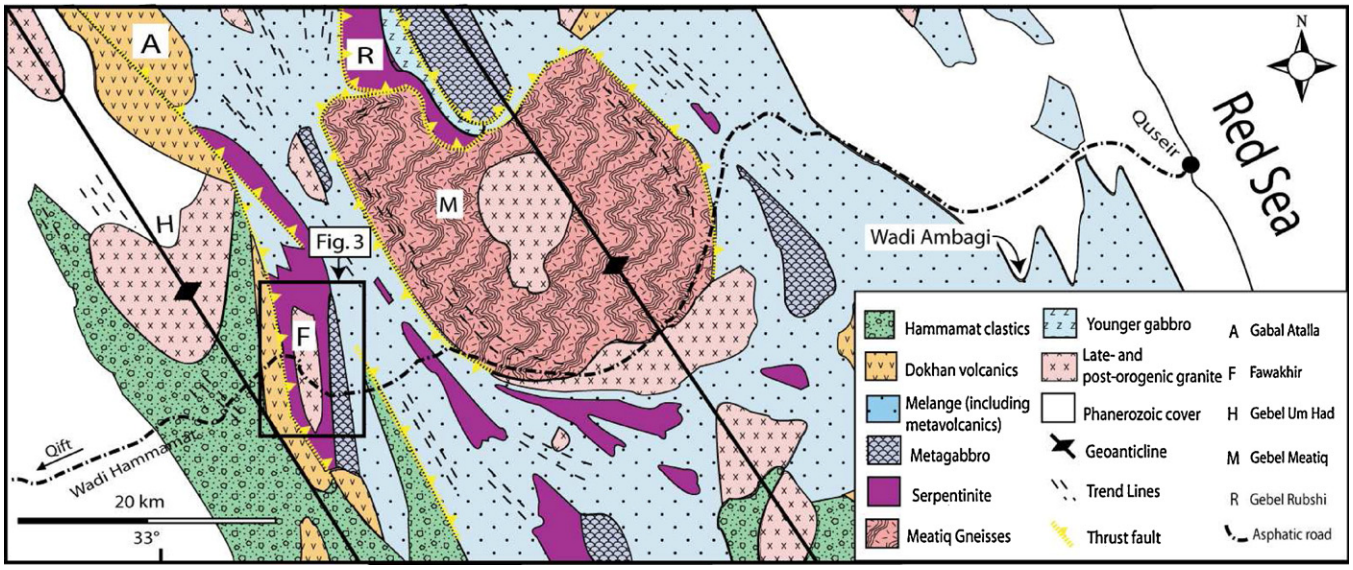

Fig. 2. Simplified geological map of the Qift-Quseir road outlined by rectangle in Fig. 1b. Modified from El-Gaby et al. (1984).

The basal ultramafic rocks are intruded by the Fawakhir Monzodiorite which has an emplacement age of 597.8 ± 2.9 Ma (Andresen et al., 2009). Andresen et al. (2009) reported a crystallization age of 736.5 ± 1.2 Ma for zircons from an ophiolitic gabbro of the Fawakhir area.

Ultramafic rocks have been severely serpentinized. The serpentinite is characterized by a mesh texture and is crosscut by many shear zones along which it is altered to talc and carbonates (Fig. 4a). Some pyroxenite bodies occur as irregular coarse-grained lenses within the serpentinite close to the ophiolitic gabbros.

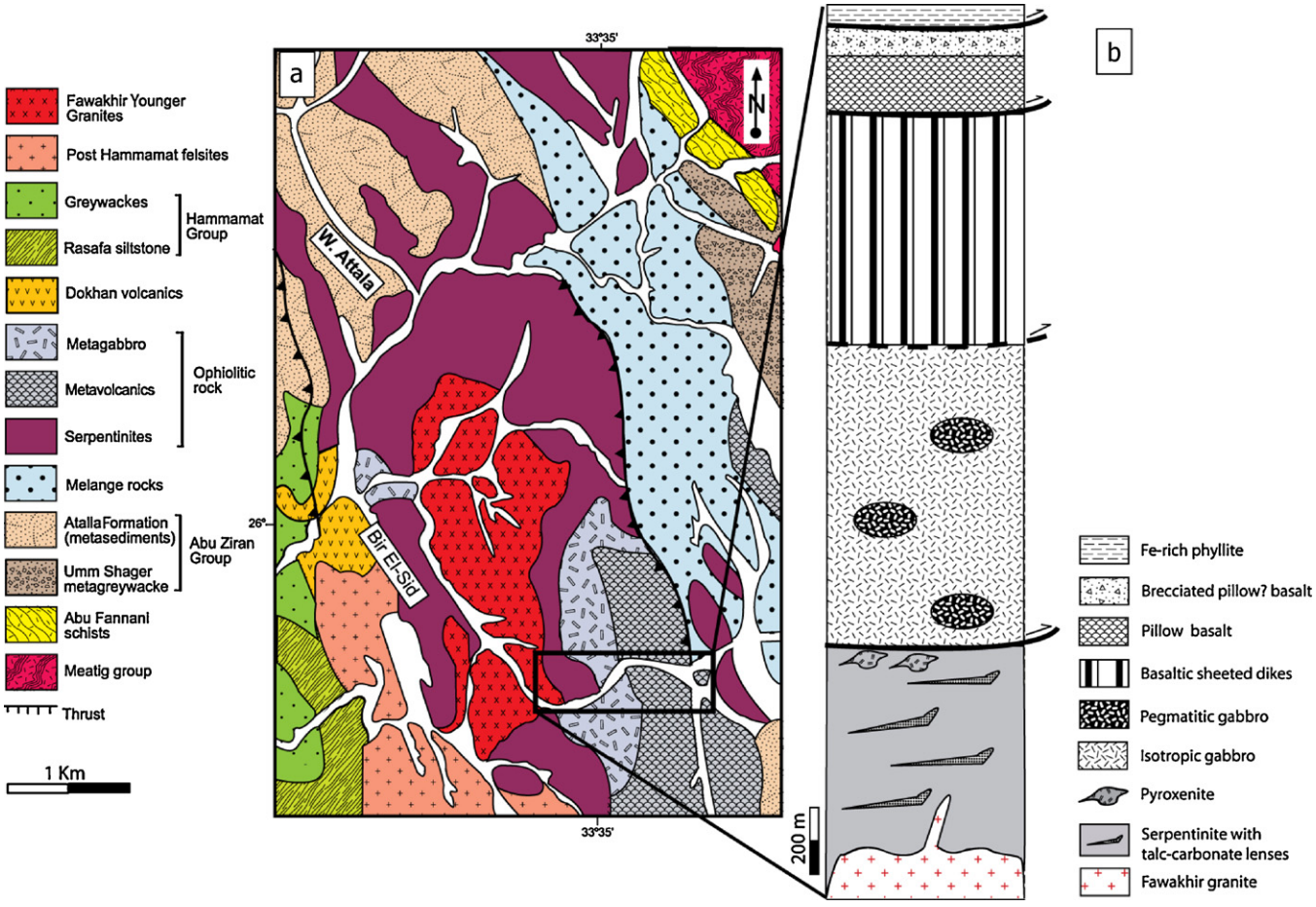

Fig. 3. (a) Geological map of the Fawakhir area outlined by the rectangle in Fig. 2. Modified from El-Sayed et al. (1999). (b) Symbolic stratigraphic section showing the main rocks units of the Fawakhir ophiolite.

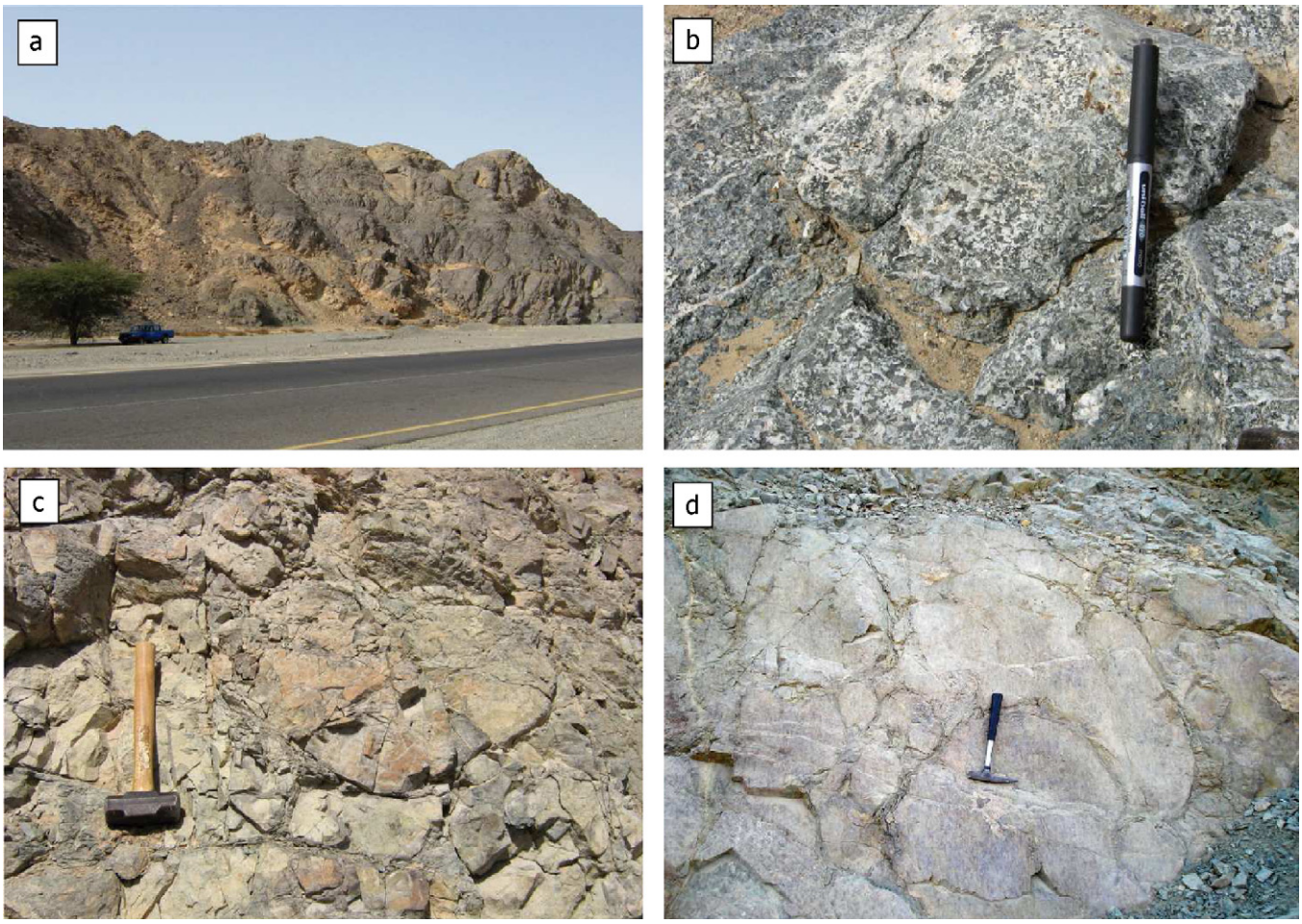

Fig. 4. Field photographs of the mantle and plutonic sections of the Fawakhir ophiolite. (a) Massive serpentinite altered to talc-carbonate (buff colour) along localized shear zone. (b) Ophiolitic isotropic gabbro. (c) Highly jointed pillow basalt of the Fawakhir ophiolite. (d) Large pillow lava enclosing smaller one of the eastern mélange. (For interpretation of the references to colour in this figure legend, the reader is referred to the web version of the article.)

Gabbro is the most abundant rock type in the Fawakhir ophiolite and is best observed at Bir El-Sid. It is mostly isotropic (Fig. 4b) with its grain size varying from coarse-grained to fine-grained from west to east. Pegmatitic gabbros and doleritic varieties occur as pockets within the isotropic gabbro. These gabbroic rocks are dissected by widespread quartz, epidote and carbonate veinlets and are intruded by rare trondhjemite veins. Isotropic gabbro grades upwards into doleritic rocks with local preservation of sheeted dike features. NW-SE-oriented sheeted dikes are ~2-m-thick on average and dip mostly to the NE. Sheeted dikes and to a lesser extent the gabbros are dissected by dike-parallel brittle fault zones that show hydrothermal alteration features. Dike-perpendicular, NE-SW-oriented brittle faults are also common within the sheeted dike complex. The entire ophiolite is intruded by less deformed, individual basaltic andesitic dikes that represent late-stage magmatism during its evolution.

Volcanic rocks display pillow structures and slightly porphyritic and amygdaloidal textures (Fig. 4c), and are highly brecciated. They are locally associated with hyaloclastites and very fine-grained red pelites. Pillow lavas also occur in the mélange along the Qift-Qusier Road close to Qusier City (Fig. 4d). There, pillow lavas display a way-up direction towards the southeast and are unconformably overlain by Miocene sedimentary rocks to the west.

4. Petrography

The mineralogical characteristics of the Fawakhir ophiolite and Qift-Qusier mélange are summarized in Table 1. Pyroxenite is strongly altered to talc, serpentine and tremolite with some clinopyroxene relics. The outlines of completely altered pyroxene crystals can be seen through the alignment of iron oxides along the cleavage planes mimicking a bastite texture (Fig. 5a). Large talc flakes retain the original outlines of the pyroxene crystals, exhibiting a mosaic seriate texture. Small talc crystals aggregate with serpentine and tremolite. Some of the pyroxenite bodies contain less altered plagioclase crystals. Gabbros in the Fawakhir area are medium to coarse-grained comprising plagioclase, amphibole (mostly actinolite), and subordinate augite relics, mainly in the core of hornblende, with accessory apatite and opaque minerals (Fig. 5b). In addition to actinolite, chlorite, epidote, sericite, calcite and titanite are uncommonly recorded as secondary minerals in the order of decreasing abundance.

Dolerites and pillow lavas are characterized by medium and fine-grained crystals respectively. Medium-grained dolerites are intergranular (Fig. 5c) and locally porphyritic. Plagioclase and chloritized pyroxene phenocrysts are set in a groundmass of fine-grained plagioclase, actinolite, chlorite, epidote, and titanite. Chlorite, actinolite, and epidote are alteration products of pyroxene interstitial to plagioclase laths forming an intersertal texture. Pillow basalts have the same mineralogical composition as dolerites; however, they are mostly aphanitic. In addition to the intersertal texture, plagioclase laths of the pillow lavas locally display a variolitic texture and epidote forms aggregates of pseudo-phenocrysts (Fig. 5d). Pillow basalts in the eastern mélange are weakly porphyritic. The phenocrysts are long thin turbid plagioclase that might have resulted from quenching (Fig. 5e). In the vicinity of

Table 1
Mineralogical composition of Qift-Qusier ophiolitic rocks.

Lithology	Mineral assemblage
Pyroxenites	Clinopyroxene (relics) + talc + tremolite ± serpentine ± plagioclase ± opaques
Gabbros	Plagioclase + augite + hornblende + actinolite + chlorite ± epidote ± sericite ± calcite ± titanite ± opaques
Sheeted dikes and pillow lavas	Plagioclase + chlorite + actinolite + epidote ± titanite
Actinolite schists	Actinolite + plagioclase ± quartz ± epidote ± opaques
Late dikes	Plagioclase + hornblende + chlorite ± quartz ± epidote ± apatite ± opaques

the Meatiq gneissic dome the igneous textures are partly obscured, and the mélange volcanic rocks grade into actinolite schist with the increasing intensity of deformation.

The younger, post-ophiolitic dikes intruding the Fawakhir ophiolite are composed of basaltic andesite to andesite, which are locally porphyritic including amphibole and plagioclase phenocrysts (Fig. 6f). The groundmass is composed largely of plagioclase and hornblende with subordinate amount of biotite and quartz. Hornblende is euhedral and brown. The main alteration mineral assemblage includes chlorite, sericite, epidote, and calcite in the order of decreasing abundance. Iron oxides and apatite are the main accessory minerals.

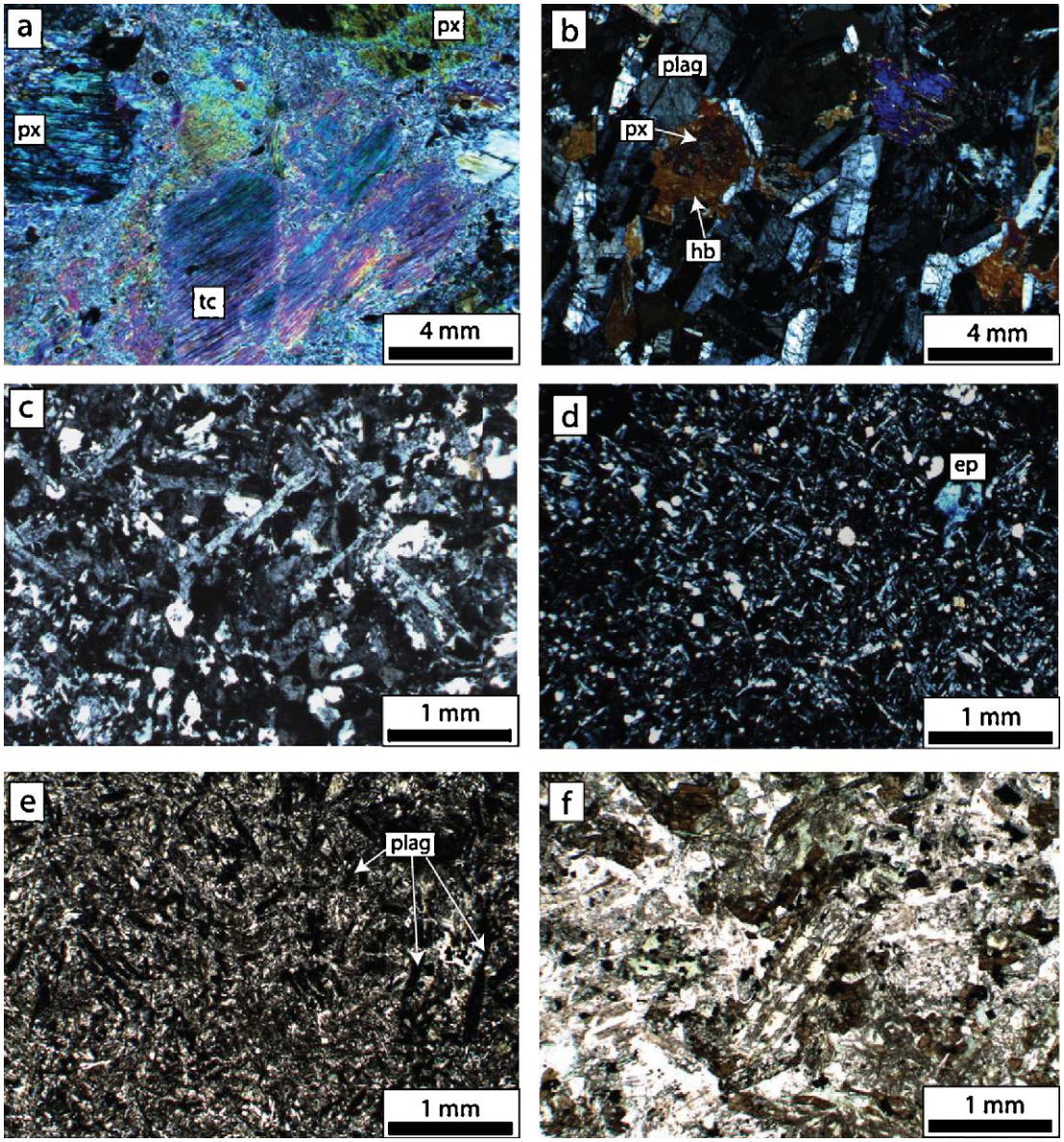

Fig. 5. Photomicrograph of the Fawakhir ophiolite and the mélange fragments. (a) Pyroxene (px) altered to talc (tc) and the iron oxide arranged along the cleavage in the pyroxenite of the Fawakhir area (XPL). (b) Plagioclase (plag) and hornblende (Hb) association in the gabbro of the Fawakhir ophiolite with pyroxene (px) relict in the core (XPL). (c) Doleritic texture of the sheeted dikes complex of the Fawakhir ophiolite (XPL). (d) Intergranular plagioclase laths of the pillow lava, of the Fawakhir ophiolite, enclosing epidote pseudo-phenocryst (XPL). (e) Long thin turbid plagioclase microphenocryst with the finer plagioclase laths of the pillow lava of the eastern mélange blocks (PPL). (f) Porphyritic andesite with chloritized brown hornblende of the calc-alkaline dike cutting ophiolitic rocks (PPL). XPL, crossed polarized light. PPL, plane polarized light.

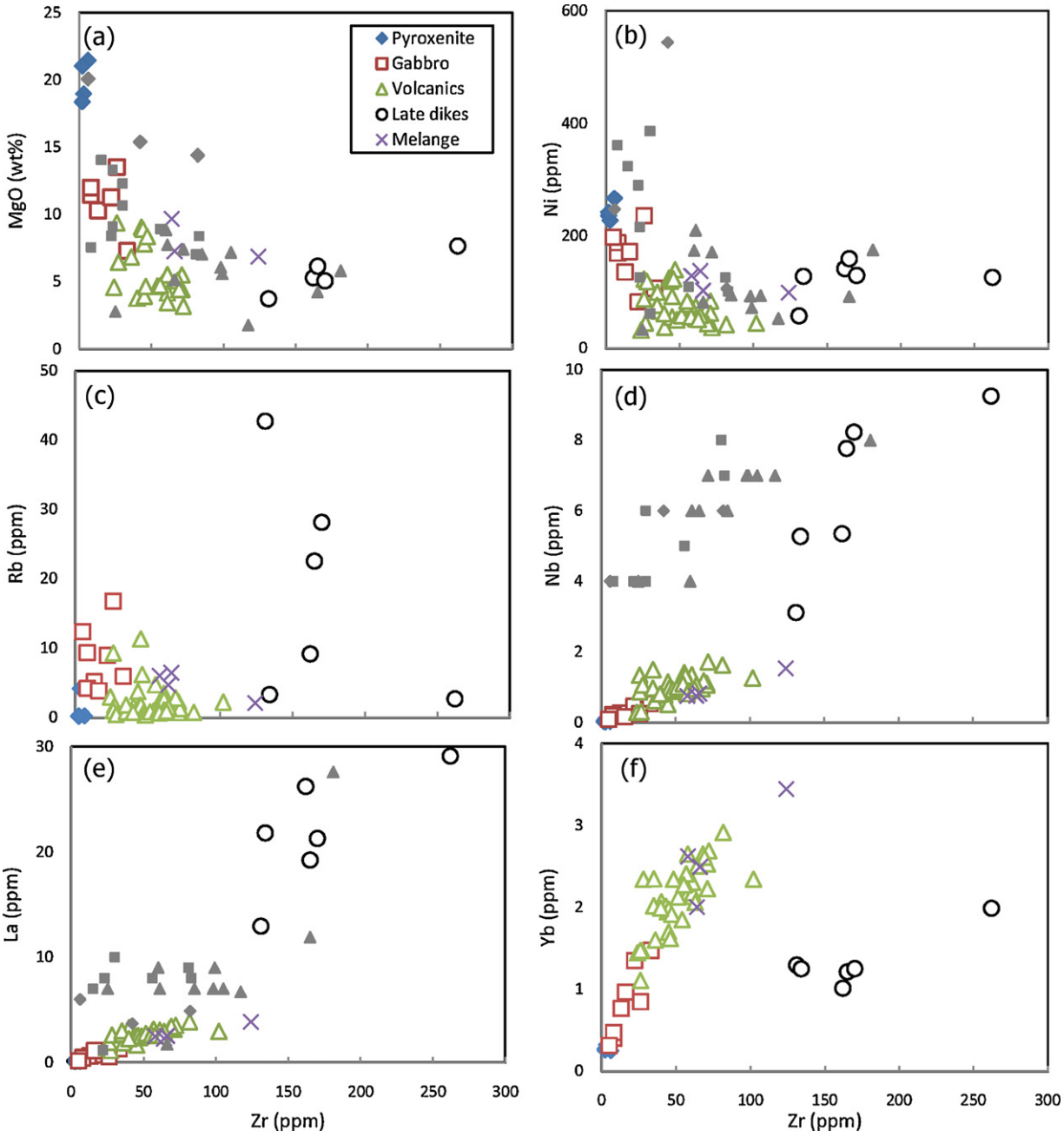

Fig. 6. Variation diagrams of Zr versus major and trace elements: (a) MgO, (b) Ni, (c) Rb, and (d) Nb, (e) La, and (f) Yb of the Fawakhir ophiolite and late dikes and the eastern mélange rocks. (The grey diamond, square, and triangle symbols are the ophiolitic boninitic gabbro, gabbros, and volcanics respectively from El-Sayed et al., 1999.)

5. Analytical methods

Whole-rock samples were crushed in a hydraulic press and then pulverized using an agate mill in the Department of Earth and Environmental Sciences, University of Windsor, Canada. Samples were analyzed for both major and trace elements. Major elements were analyzed by Thermo Jarrell-Ash Enviro II ICP at ACTLABS, Ancaster, Canada. Samples were fused with a flux of lithium metaborate and lithium tetraborate in an induction furnace. The melt was immediately mixed with 5% nitric acid containing an internal standard until completely dissolved. Totals of major element oxides are 100 ± 1 wt% and the analytical precisions for major elements are 1–2%. Standards, DNC-1 and BIR-1, were used as international references to estimate accuracy of the major elements (Supplementary materials).

Samples were analyzed for rare earth elements (REE), high field strength elements (HFSE), large ion lithophile elements (LILE) and transition metals (Ni, Co, Cr and V) by a high-sensitivity Thermo Elemental X7 ICP-MS at the Great Lakes Institute for Environmental Research (GLIER), University of Windsor, Canada, using the protocol of Jenner et al. (1990). For sample dissolution, 100–130 mg of powder was dissolved in concentrated $HF–HNO_3$ mixture in screw-top Teflon (Savillex®) bombs at a temperature of ~120 °C for three days until no residue was visible. The sample was further attacked with concentrated $HNO_3–H_3BO_3–H_2C_2O_4$ and then twice with 50% HNO_3. Standards, BHVO-1 and BHVO-2, were used as international reference materials to estimate accuracy of the measured trace elements (Supplementary materials). Analytical precisions are estimated as follows: 1–10% for REE, Rb, Sr, Ba, Y, Nb, Co, Cu, Zr, and U; 10–20%

Table 2
Summary of major (wt%) and trace (ppm) elements concentrations and significant element ratios for the Wadi Ghadir ophiolitic complex and associated dikes.

	Pyroxenites	Gabbros	Volcanic rocks	Late dikes	Mélange blocks
SiO_2	51.2–55.5	42.1–51.5	51.1–66.0	52.5–62.5	49.8–56.2
Al_2O_3	2.8–9.6	15.0–18.9	13.1–16.5	14.6–17.6	14.0–17.2
$Fe_2O_3^t$	7.8–9.8	6.3–14.0	6.6–11.7	5.4–10.1	9.5–13.4
MgO	18.4–21.5	7.3–13.5	3.2–9.4	3.7–7.7	4.8–9.7
CaO	9.4–16.0	11.8–15.4	3.0–10.8	5.4–8.3	8.0–11.8
TiO_2	0.07–0.10	0.15–0.73	0.40–1.18	0.87–1.82	0.83–1.86
Mg-number	79–84	61–77	38–66	52–60	50–66
Cr	411–558	83–314	7–205	34–94	99–473
Sc	61–72	37–47	25–40	14–23	35–47
V	175–193	87–295	87–390	105–208	120–370
Co	54–69	33–49	18–57	19–41	40–45
Ni	228–267	83–198	32–140	58–159	99–138
Th	0.06–0.14	0.09–0.32	0.22–0.76	2.39–3.96	0.25–0.42
Y	1.78–2.28	2.55–13.8	9.11–26.5	13.7–23.9	20.7–31.6
Zr	2–6	5–33	24–102	131–262	58–124
Nb	0.02–0.05	0.09–0.53	0.31–1.72	3.12–9.25	0.75–1.53
La	0.07–0.14	0.17–1.3	1.14–3.88	19.2–29.1	2.27–3.86
Nd	0.22–0.34	0.9–3.67	2.9–7.56	15.4–40.4	7.23–11.2
Sm	0.12–0.15	0.2–1.34	0.97–2.52	3.37–8.7	2.57–3.79
Gd	0.22–0.26	0.34–2.03	1.33–3.81	3.21–7.56	3.4–5.13
Yb	0.25–0.32	0.4–1.47	1.11–2.65	1.01–1.99	2–3.44
Zr/Nb	94–326	36–105	19–83	21–48	77–85
La/Yb_{cn}	0.15–0.38	0.38–0.86	0.56–1.19	7.17–18.6	0.67–0.81
La/Sm_{cn}	0.3–0.61	0.4–1.06	0.65–1.22	2.13–2.48	0.52–0.66
Gd/Yb_{cn}	0.67–0.79	0.85–1.14	0.89–1.23	2.04–4.25	1.23–1.41
Eu/Eu*	0.93–1.41	0.85–1.48	0.77–1.65	0.86–1.02	0.94–0.98

for V, Ni, Zn, Cs, Mo, and Ga; and 20–30% for Ta, Th, Cr, and Pb.

Major element analyses are recalculated to 100 wt% anhydrous basis and all Fe set as Fe^{2+}. Mg-numbers (%) were calculated as the molar ratio of $100 \times Mg/(Mg + Fe^{2+})$ after Ragland (1989). Chondrite (cn) and primitive mantle (pm) compositions derived from Sun and McDonough (1989) and Hofmann (1988) respectively. Europium (Eu/Eu*) and cerium (Ce/Ce*) anomalies were calculated with respect to neighboring REE (Rollinson, 1993).

6. Geochemical results

Geochemical data for the Fawakhir pyroxenites, gabbros, volcanic rocks, and dikes, and for samples from the mélange along Qift-Qusier Road are presented in Table 2 and supplementary materials.

6.1. Pyroxenites and gabbros

Pyroxenites are characterized by 51–56 wt% SiO_2, MgO = 18–22 wt% and Al_2O_3 = 3–9 wt% (Fig. 6a and Table 2). Gabbros have lower silica (SiO_2 = 42–52 wt%) and MgO (MgO = 7–14 wt%) values but higher Al_2O_3 (Al_2O_3 = 15–19 wt%) than pyroxenites. Pyroxenites also have lower TiO_2 (0.07–0.1 wt%) than gabbros (0.15–0.73 wt%). In terms of Al_2O_3/TiO_2, both pyroxenites (35–91) and gabbros (21–113) show wide ranges and overlapping ratios. Pyroxenites have higher concentrations of compatible elements (Cr = 411–558 ppm, Co = 54–69 ppm, Sc = 61–72 ppm) than gabbros (Cr = 83–314 ppm, Co = 33–49 ppm, Sc = 37–47 ppm), but Ni concentrations overlap between the two groups (Fig. 6b). On the other hand, gabbros have higher concentrations of the incompatible elements (LILE, HFSE, REE) than pyroxenites (Table 2).

Pyroxenites display LREE-depleted patterns (La/Sm_{cn} = 0.30–0.61; La/Yb_{cn} = 0.15–0.38) accompanied by low REE abundances. Their HREE patterns (Gd/Yb_{cn} = 0.67–0.79) are negatively fractionated (Fig. 7). Gabbros have similar REE patterns to pyroxenites but are less depleted in LREE (La/Sm_{cn} = 0.40–1.06; La/Yb_{cn} = 0.33–0.86), their HREE patterns (Gd/Yb_{cn} = 0.85–1.14) are near-flat and their REE abundances are higher (Fig. 7a and Table 2). Europium anomalies vary from slightly positive to slightly negative in both rock types. Primitive mantle-normalized patterns for both rock types are characterized by enrichment of Ba and Th (LILE) over HFSE (Zr, Ti, Y) and HREE. Both rock types have large negative Nb anomalies (Fig. 8).

6.2. Volcanic rocks

Volcanic rocks of the Fawakhir ophiolite are characterized by MgO = 3–9 wt%, Ni = 32–140 ppm and Cr = 7–205 ppm (Table 2). Mg-numbers (38–66) are generally lower than those of the gabbros (Table 2). Similarly, concentrations of TiO_2 (0.40–1.18 wt%), Zr (24–102 ppm), and Y (9.11–26.5 ppm) are lower than those of the gabbros (Table 2).

Volcanic rocks display moderately depleted to slightly enriched LREE patterns (La/Sm_{cn} = 0.65–1.22, La/Yb_{cn} = 0.56–1.19) (Fig. 7b and Table 2). The HREE are moderately fractionated (Gd/Yb_{cn} = 0.89–1.23) (Fig. 7b). The primitive mantle-normalized trace element patterns of the volcanic rocks are characterized by negative Nb anomalies and variable enrichment of Ba and Th (LILE) over HFSE (Fig. 8b).

6.3. Mélange blocks

Major and trace element contents of the blocks of volcanic rocks from the mélange unit to the west of Qift-Qusier Road overlap with those of the volcanic rocks of the Fawakhir ophiolite (Table 2). These mélange volcanic rocks are characterized by MgO = 5–10 wt%, Ni = 99–138 ppm, Cr = 99–473 ppm and Mg-number = 50–66 that are slightly higher than those of the ophiolitic volcanic rocks (Table 2). In contrast, Al_2O_3/TiO_2 ratios of the ophiolitic volcanic rocks (13–34) are higher than those of volcanic rocks in the mélange (8–14). Despite an overlap in composition between the ophiolitic volcanic rocks and the volcanic blocks in the mélange, the TiO_2 (0.83–1.86 wt%), Zr (58–124 ppm) and Y (20.7–31.6 ppm) concentrations of the latter group are higher (Table 2 and Fig. 6).

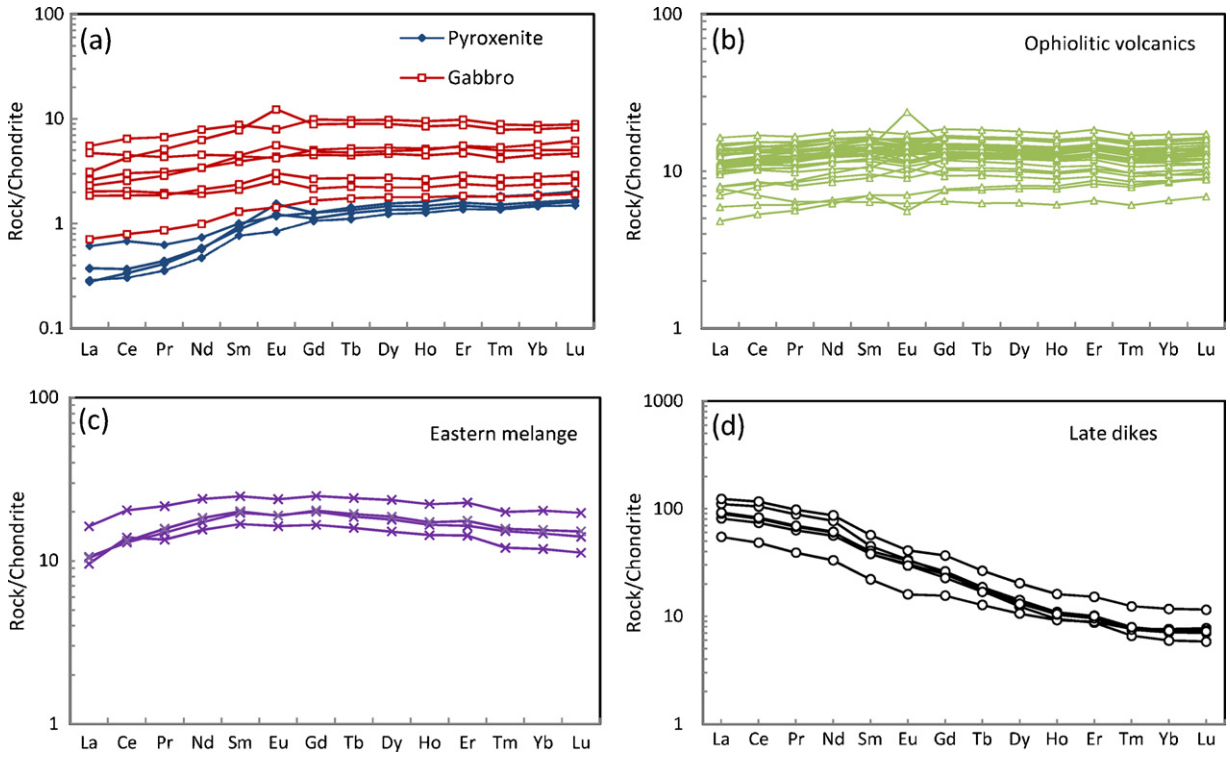

Fig. 7. Chondrite-normalized REE patterns for (a) ophiolitic pyroxenite and gabbros, (b) ophiolitic pillow lavas, (c) eastern mélange volcanic blocks, and (d) calc-alkaline dikes. Chondrite normalization values are from Sun and McDonough (1989).

REE patterns (La/Sm_{cn} = 0.52–0.66, La/Yb_{cn} = 0.67–0.81) of the volcanic blocks in the mélange are similar to those of their ophiolitic counterparts (Fig. 7). All volcanic blocks in the mélange have positively fractionated HREE patterns (Gd/Yb_{cn} = 1.23–1.41) (Fig. 7c). Volcanic rocks both in the ophiolite and the mélange are characterized by negative Nb anomalies and minor enrichment of Ba and Th (LILE) over HFSE (Fig. 8c).

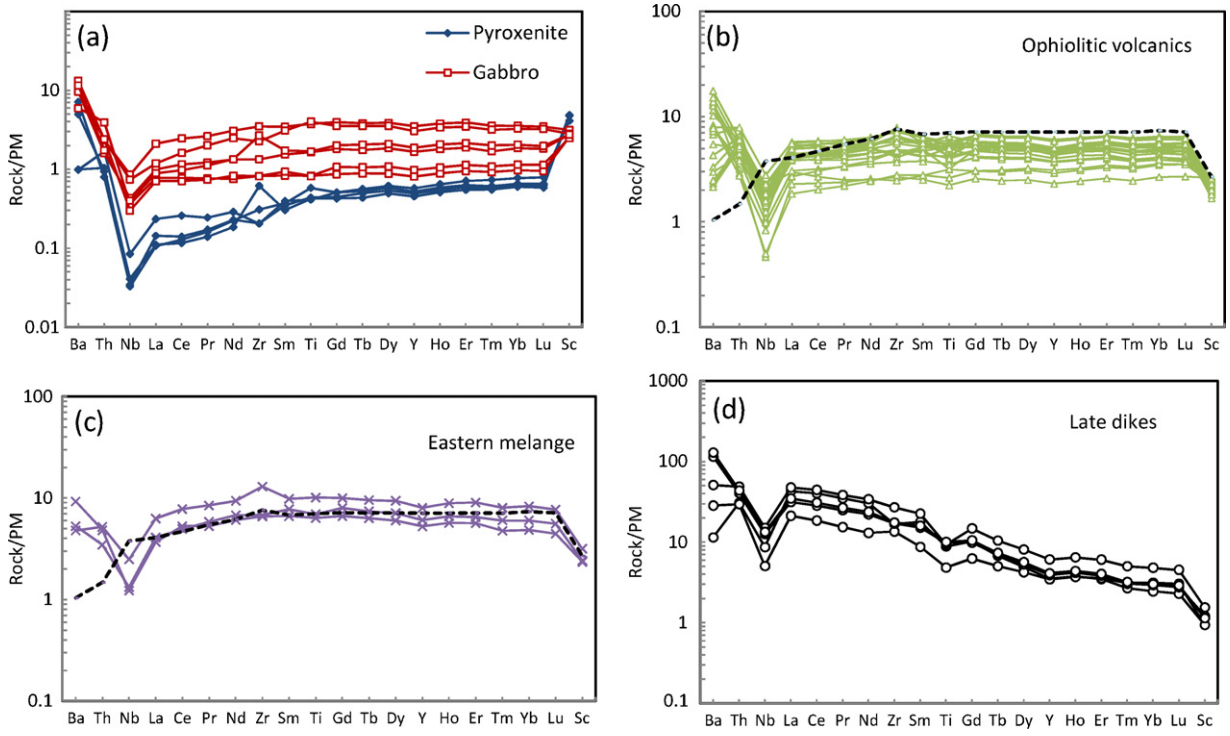

Fig. 8. Primitive mantle-normalized trace elements patterns for (a) ophiolitic pyroxenite and gabbros, (b) ophiolitic pillow lavas, (c) eastern mélange volcanic blocks, and (d) calc-alkaline dikes. Primitive mantle normalization values are from Hofmann (1988). Dashed line represents N-MORB. N-MORB values are from Sun and McDonough (1989).

6.4. Late dikes

The late, post-ophiolitic dikes are characterized by MgO (4–8 wt%), Cr (34–94 ppm), and Ni (58–159 ppm) concentrations similar to those of the ophiolitic volcanic rocks (Table 2). These calc-alkaline dikes are enriched in TiO_2 (0.87–1.82 wt%), Zr (131–262 ppm) and most of the LILE over the ophiolitic volcanic rocks. Their REE patterns show pronounced positive fractionation of REE where La/Yb_{cn} = 7.17–18.6, La/Sm_{cn} = 2.13–2.48, and Gd/Yb_{cn} = 2.04–4.25 (Fig. 7d). The primitive mantle-normalized trace element patterns are characterized by negative Nb anomalies, small negative Ti anomalies, and enrichment of LILE and Th over the rest of the HFSE (Fig. 8d).

7. Discussion

7.1. Alteration

Ophiolites are variably altered and metamorphosed through seafloor hydrothermal circulation systems and during obduction/accretion-related processes (see Gillis and Banerjee, 2000; Furnes et al., 2000). Ophiolitic rocks of the Fawakhir area and in the eastern mélange underwent various degrees of post-magmatic alteration. Although the original igneous textures are well preserved in the Fawakhir ophiolite, the mineralogical compositions of these rocks have been largely changed. The primary pyroxene and plagioclase were altered to actinolite, chlorite, epidote, albite, and titanite. Volcanic rocks are more extensively altered than the gabbros.

Given that the Fawakhir ophiolite was metamorphosed at greenschist facies, the primary geochemical characteristics of its rock units might have been changed. Alteration criteria proposed by Polat and Hofmann (2003) are used to assess the element mobility during post-magmatic alteration. Different major and trace elements are plotted against Zr (Fig. 6), which is one of the least mobile elements under various alteration processes (Winchester and Floyd, 1977). Among the major elements, MgO, Al_2O_3, and CaO show a moderate correlation with Zr abundances and TiO_2, P_2O_5, Ni, Cr, Sc, Co, Th, REE (La, Sm, Yb) and HFSE (Y, Nb) correlate well with Zr abundances (Fig. 9). The strong correlation with Zr indicates that these elements were not significantly mobile during post-magmatic alteration. In contrast to these immobile elements, K_2O and LILE (Rb, Ba, Sr) are not correlated with Zr, pointing to their mobility during alteration (Fig. 8c).

The relative immobility of REE and HFSE is confirmed by the coherent chondrite-normalized REE patterns and primitive mantle-normalized extended trace element patterns for different groups of samples (Figs. 7 and 8). Although the LILE (Ba) of the volcanic rocks shows a large variation in their primitive mantle-normalized patterns, the LILE (Ba) patterns of the gabbroic rocks are more coherent (Fig. 8a). This may have been resulted from the mobility of LILE in the extrusive rocks during ocean floor hydrothermal alteration; however, the circulating hydrothermal fluids may not have penetrated deep into the gabbros to affect their LILE concentrations. Even the most-deformed gabbro sample (EGY-06-19) still displays a coherent HREE pattern as the other gabbroic rocks, indicating that LREE are more susceptible to mobility during intense alteration than HREE, in accordance with the findings of Humphries (1984). Samples with variably negative and/or positive Ce anomalies ($0.9 > Ce/Ce^* > 1.1$) were designated as variably altered and were not used in our petrogenetic interpretations (see Polat and Hofmann, 2003). Most samples do not show any significant Ce anomalies. Sample EGY-04-01 is an outlier and has a small positive Ce anomaly ($Ce/Ce^* = 1.22$), but its chondrite- and primitive mantle-normalized patterns are comparable to those of unaltered samples collected from the same outcrop.

In summary, concentrations of most elements, except the LILE, in the Fawakhir ophiolite were not significantly disturbed by post-magmatic alteration processes. The mobility of LILE under most alteration conditions and the relatively immobile nature of the REE and HFSE agree with the results of other studies on variably altered rocks (Winchester and Floyd, 1977; Humphries, 1984; Ordóñez-Calderón et al., 2008; Gardien et al., 2008).

7.2. Chemical classification and magma series

Using the Zr/TiO_2–Nb/Y classification diagram of Winchester and Floyd (1977), all rock types can be classified as sub-alkaline ($Nb/Y < 0.67$) where the gabbros and volcanic rocks plot mostly in the basalt and andesite-basalt field (Fig. 9a). On the Zr versus Y diagram, all the ophiolitic rocks and volcanic blocks in the mélange plot in the tholeiitic field but the post-ophiolitic dikes plot in the calc-alkaline field (Fig. 9b). However, using the SiO_2 versus FeO^*/MgO diagram, the Fawakhir ophiolite plot mostly with the younger, post-ophiolitic dikes in the calc-alkaline field whereas the volcanic blocks in the mélange extend to the tholeiitic field (Fig. 9c). Recently, Arculus (2003) raised the question over use of the term "calc-alkaline" in multiple ways. These diagrams are used to identify different magma series rather than identifying calc-alkaline rocks that would indicate convergent margin tectonic setting. Four magma series have been identified by this study (Fig. 9c). The younger post-ophiolitic dikes crosscutting the Fawakhir ophiolite and the mélange are distinguished by their high Zr/Y (>7) ratios and show no iron enrichment. The mélange samples follow the high-Fe tholeiitic trend of Arculus (2003). Most of the ophiolitic gabbros and volcanic rocks follow an iron enrichment trend that extends along the boundary between low-Fe and medium-Fe fields (Fig. 9c). The pyroxenites of the Fawakhir ophiolite show no iron enrichment along with the boninitic gabbros reported by El-Sayed et al. (1999) in the Fawakhir ophiolite. The correlation between Zr and TiO_2 confirms the subdivision into compositional groups indicated by SiO_2 versus FeO^*/MgO (Fig. 9d).

7.3. Fractional crystallization and partial melting

In this section, we evaluate qualitatively the variations in the whole-rock chemistry of the Fawakhir ophiolitic gabbros and volcanic rocks and of the volcanic rocks in the mélange as a result of fractional crystallization and partial melting processes. The relationship between pyroxenites and older ophiolitic rocks will be discussed in the next section. Tatsumi and Eggins (1995) used the FeO^*/MgO ratio (<1) and Mg-number (>70) as criteria to identify the potential primitive magmas. The Fawakhir volcanic rocks have FeO^*/MgO less than one (Fig. 9c), and low Mg-number (38–66). In addition, the Fawakhir ophiolitic rocks have low Cr (7–314 ppm) and Ni (32–198 ppm) contents. The low abundances of the mantle-compatible elements indicate that the ophiolitic magmas were not in equilibrium with mantle residue (Smith et al., 1997). The evolved nature of the Fawakhir ophiolitic rocks suggests that fractional crystallization played a major role in the evolution of their magmas. Plots of Zr, which is an immobile and highly incompatible fractionation index, versus selected major and trace elements are used to assess the role of fractional crystallization. Variations in the abundance of these elements relative to Zr may indicate a co-genetic origin and chemical evolution through fractional crystallization (Fig. 6).

The Zr contents range from 5 to 33 ppm in gabbros and from 24 to 102 ppm in volcanic rocks, whereas the Zr content of the volcanic blocks in the mélange ranges from 58 to 124 ppm. The negative correlation between MgO and Ni versus Zr may indi-

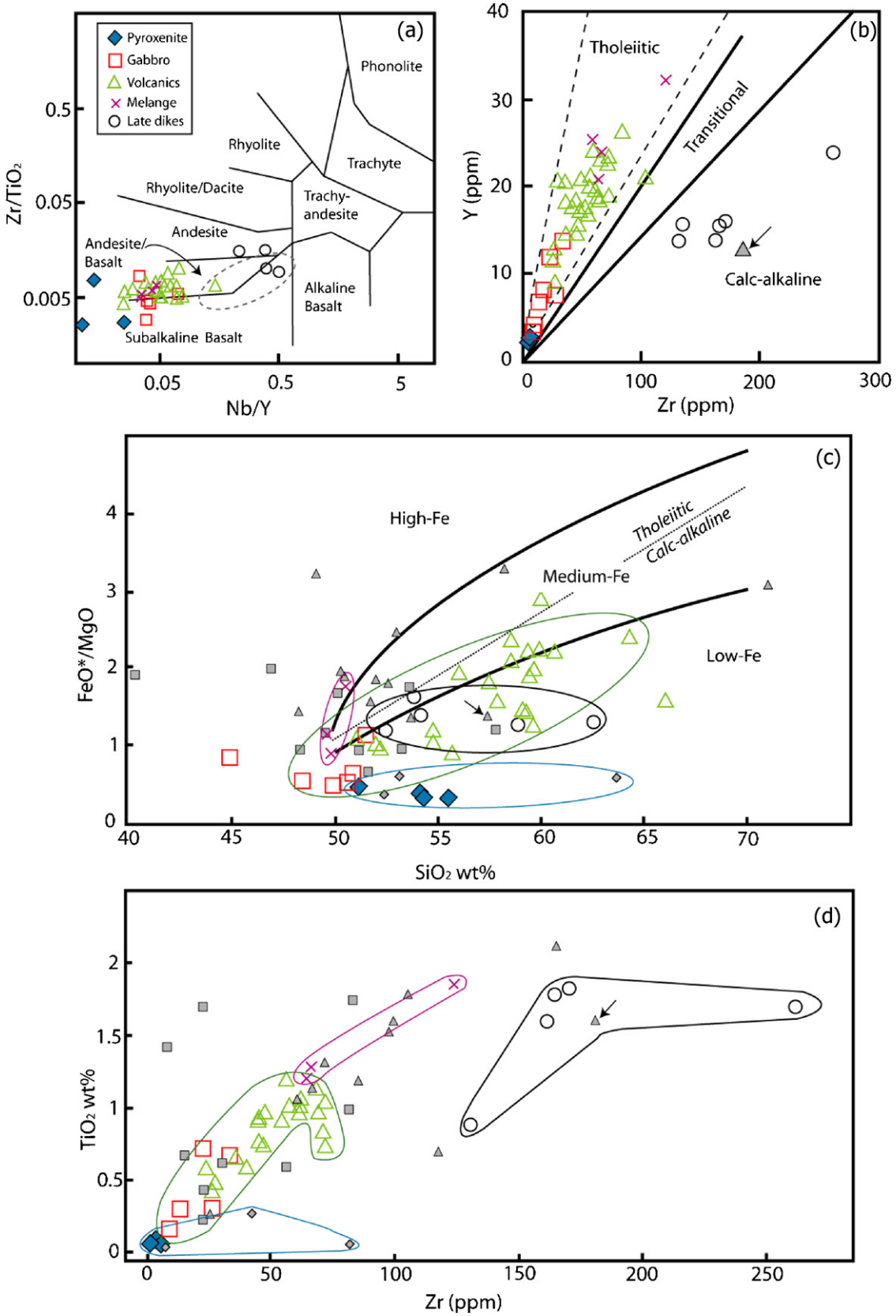

Fig. 9. (a) Zr/TiO_2 versus Nb/Y diagram of Winchester and Floyd (1977) for the ophiolitic rocks, the eastern mélange rocks and younger dikes. (b) Zr versus Y diagram of Barrett and MacLean (1994) to distinguish the magma series of the different rocks types. (c) SiO_2 versus FeO^*/MgO diagram showing four magma series, the dotted line from Miyashiro (1974) and the bold lines are from Arculus (2003). (d) Zr versusTiO_2 variation diagrams. (Dashed line fields in a and b are the gabbros and volcanics of the Fawakhir ophiolite. The grey diamond, square, triangle symbols in c are the ophiolitic boninitic gabbro, gabbros, volcanics respectively. The grey triangle with arrow is MV-33 from El-Sayed et al., 1999 as the rest.)

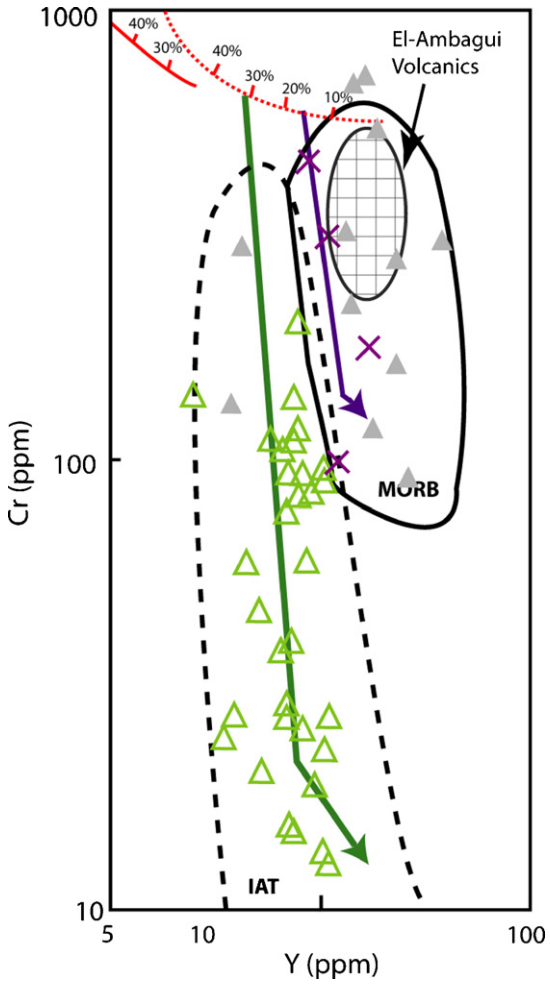

Fig. 10. Cr versus Y discrimination diagram (Pearce et al., 1984) for the Fawakhir ophiolite, calc-alkaline dikes and eastern mélange blocks. The arrows are qualitative fractional crystallization trends (parallel to fractional crystallization trends of Pearce, 1982) for the Fawakhir ophiolitic volcanic rocks (green) and eastern mélange pillow lava (purple). The red lines are partial melting trends of primordial mantle (dotted red line) and depleted mantle (solid red line) from Pearce et al. (1984). (El-Ambagui field from El-Mahallawi, 1994; symbols as Fig. 9). (For interpretation of the references to colour in this figure legend, the reader is referred to the web version of the article.)

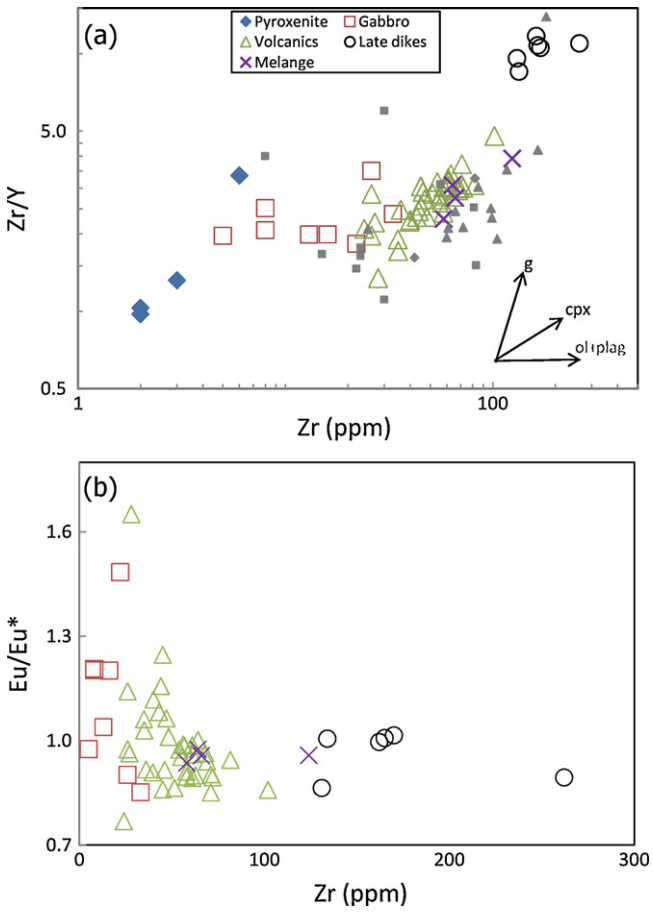

Fig. 11. (a) Zr versus Zr/Y diagram with fractionation trends of olivine (ol) and plagioclase (plag), clinopyroxene (cpx), and garnet (g). Fractionation trends from Pearce and Norry (1979). (b) Zr versus Eu/Eu* diagram.

cate the early crystallization of olivine from the ophiolitic magmas (Fig. 6a and b). On the Cr versus Y diagram (Pearce, 1982), the ophiolitic rocks plot parallel to the Cr axes indicating the early crystallization of Cr-spinel (Fig. 10). Olivine and Cr-spinel were reported as a cumulus phase in the peridotites of the Fawakhir area by Nasseef et al. (1980). Crystallization of olivine and Cr-spinel was followed by clinopyroxene and plagioclase (Fig. 11a). On the Zr/Y versus Zr diagram, the ophiolitic gabbros follow mainly the olivine and plagioclase fractionation trend (see Pearce and Norry, 1979; Magganas, 2002). The ophiolitic volcanic rocks have a wider range of Zr/Y, which can be attributed to pyroxene fractionation. Europium anomalies display some variations between the ophiolitic rocks. On the Zr versus Eu/Eu*, the Eu anomalies range mainly from positive in the least evolved gabbroic rocks to negative in the fractionated volcanic rocks (Fig. 11b), probably indicating plagioclase fractionation. Plagioclase fractionation results in a systematic decrease in Al_2O_3 from the gabbros to volcanic rocks. The Fawakhir ophiolic rocks show a consistent increase of TiO_2 from 0.15 to 0.73 wt% in gabbros and up to 1.18 wt% in the volcanic rocks. The fractional crystallization of the Fe–Ti oxide phase appears to have taken place at the late stage. This is indicated by the decrease of the TiO_2 content in the evolved ophiolitic volcanic rocks on the Zr–TiO_2 variation diagram (Fig. 9d).

Assessment of the role of fractional crystallization in the magmatic evolution of the volcanic blocks in the mélange is difficult due to the limited number of samples. However, the possible influence of fractional crystallization can still be detected through the range of Zr content (58–124) and Mg-numbers (50–66) of these rocks. In comparison with the Fawakhir ophiolitic rocks, Zr and Mg-numbers in the mélange blocks have a smaller range, indicating limited effects of fractionation in their formation. Variations on the Cr versus Y and Zr/Y versus Zr diagrams of these samples suggest that olivine, Cr-spinel and clinopyroxene were the main fractionating phases (Fig. 10).

Irrespective of the mechanism of partial melting, the Cr versus Y plot can provide some information on the degree of partial melting (see Pearce et al., 1984). Extrapolation line passing through the volcanic rocks of the Fawakhir ophiolite intersects the partial melting path of the primordial mantle at a point of 30–35% of partial melting. The line of fractionation of the volcanic rocks in the mélange intersects the same partial melting curve at about 15%. As the partial melting curve calculation depends on the primordial mantle composition (Pearce, 1982), the amount of melt fraction represents the maximum tentative value. El-Sayed et al. (1999) suggested that the melting proportions of the Fawakhir ophiolite might range from 10 to 35% covering the degrees of partial melting of the Fawakhir ophiolite and the volcanic blocks in the eastern mélange as suggested by our study. The inferred high degrees of partial melting might have resulted from introduction of hydrous fluxes derived from a subducted slab. The HREE patterns and abundances (Fig. 7)

in the Fawakhir ophiolite are consistent with decompressional partial melting at a shallow depth and elevated temperatures (cf., Stern and Bloomer, 1992; Tatsumi and Eggins, 1995; Zanetti et al., 2009).

7.4. Mantle source characteristics

The geochemical characteristics of the Fawakhir ophiolite, volcanic blocks in the mélange along Qift-Qusier Road, and post-ophiolitic dikes are generally similar. Their primitive mantle-normalized patterns are systematically enriched in Th and LREE over HFSE (Nb, Zr, Y) and HREE, and exhibit pronounced negative Nb anomalies (Fig. 8). In addition to LREE, gabbros are also enriched in LILE (Fig. 8a). These geochemical characteristics are similar to those of magmatic rocks formed at convergent plate margins (cf., Pearce, 1982; Saunders et al., 1991; Hawkesworth et al., 1993). Compositions of magmatic rocks in this setting are controlled by both fluid-derived components from the subducted slab and the mantle wedge composition (Tatsumi and Kogiso, 2003). Enrichment of the LILE and Th results from the mobility of these elements during slab dehydration (Pearce and Peate, 1995). On the other hand, HFSE (Nb, Zr) and HREE tend to be less mobile than LILE and Th during dehydration processes (John et al., 2008). Thus, ratios of HFSE (Nb, Zr) and HREE in the rocks reflect their values in the mantle wedge (Pearce, 2008).

The relative contribution of both the mantle wedge and the slab-derived fluids can be assessed using M/Yb versus Nb(Ta)/Yb plots (Pearce, 1983; Pearce and Peate, 1995), where M is the incompatible element of interest (Fig. 12). On such a plot, any contribution from the slab-derived fluid of the element (M) results in displacement from the mantle array, which is defined by mantle-derived oceanic basalts (mid-ocean ridge basalts, MORB, and oceanic island basalts, OIB). For HFSE, Zr and Y, all the rock types plot within the mantle array (Fig. 12a and b), indicating that HFSE and HREE were not important components in the subduction-related flux. The ophiolitic samples and volcanic blocks in the mélange plot close to the MORB end, but the post-ophiolitic calc-alkaline dikes extend slightly towards OIB (Fig. 12). For the ophiolitic samples and mélange blocks, both LREE (La) and MREE (Sm) values are confined to the mantle array, although the LREEs plot closer to the upper boundary (Fig. 12c and d), suggesting some possible contribution from subduction-derived fluids. The calc-alkaline dikes plot above the mantle array reflecting contributions from a source other than the subduction-metasomatized mantle wedge (Fig. 12c and d). In contrast, LILE (U, Th) values are displaced above the mantle array towards higher ratios of Th/Yb and U/Yb (Fig. 12e and f), which indicate a significant contribution from the subducted slab to the mantle wedge. The dispersion of U/Yb ratios on the mantle array boundary indicates the mobility of U during later alteration. However, the consistent plot of the samples above the mantle array (Fig. 12e) indicates the contribution of the subducted slab to the mantle wedge rather than alteration as recorded by the high Th/Yb ratios. The nature of the transporting medium from the slab to the mantle wedge, either fluid or melt, influences the behavior of some elements (e.g., Zr) in a conservative or non-conservative way. Zirconium tends to behave in a non-conservative way with melting of the subducted sediment (Pearce and Peate, 1995). The restriction of Zr values of the Fawakhir ophiolitic rocks and mélange blocks to the mantle array indicates the limited role of melting of subducted sediments in the evolution of these rocks. Both the ophiolitic and mélange samples follow the low Ce/Yb trend (Hawkesworth et al., 1993). However, the post-ophiolitic dikes show slightly higher Th/Ce values relative to the Fawakhir ophiolite and mélange blocks, and thus they follow the high Ce/Yb trend (Fig. 13).

Because HFSE (Nb, Zr) and HREE are less affected by subduction-derived fluxes, they can be used to address the nature of the mantle wedge. Using HFSE and HREE ratios to assess the composition of the mantle wedge revokes the variation in the absolute concentration of HFSE that may result from pooled and fractional partial melting or from fractional crystallization (Pearce and Peate, 1995). Given that HFSE elements are conservative, they plot within the mantle array which extends from N-MORB source (lower Nb/Yb) to enriched OIB source (higher Nb/Yb). The Fawakhir ophiolitic rocks and the mélange blocks cluster around MORB values and extend towards lower Nb/Yb values (Fig. 12), which reflect the variably depleted nature of the mantle source. Melting of such a depleted source is consistent with high Zr/Nb (19–105) ratios of the ophiolitic rocks (Table 2) and resembles other variably depleted mantle sources for many arc-related rocks (cf., Davidson, 1996; Macdonald et al., 2000). Variation in the Zr/Nb ratios between the different types can be attributed to mantle heterogeneity and/or to selective tapping in the mantle column in a dynamic melting model (Pearce et al., 1995). Although post-ophiolitic calc-alkaline dikes extend slightly towards an enriched mantle source (Fig. 12), their Zr/Nb ratios (21–42) are comparable to N-MORB (N-MORB ratios = 1–39, after Sun and McDonough, 1989).

The ratios of Gd/Yb_{cn} are variable for the rock units in the study area. The Fawakhir ophiolitic rocks have almost flat HREE patterns (Gd/Yb_{cn} = 0.88–1.23; Fig. 7a and b; Table 2), which indicate a relatively shallow mantle source within the spinel stability zone. On the other hand, the mélange blocks from the eastern part of the study area show slightly higher Gd/Yb_{cn} ratios (1.23-1.41) (Fig. 7c and Table 2), reflecting either a variable contribution from a deeper garnet-bearing mantle source (>80 km) or subduction-related melt in equilibrium with eclogite (cf., Kessel et al., 2005). Another possibility to obtain a garnet signature is to melt spinel peridotite containing garnet pyroxenite veins (cf., Hirschmann and Stolper, 1996).

7.5. Pyroxenite genesis

Occurrence of pyroxenite is a common feature in many Proterozoic and Phanerozoic ophiolites. Pyroxenites occur as cumulate rocks in the transitional zone between the petrologic Moho and the seismic Moho of the ophiolitic sequence (Stern et al., 2004). The Onib ophiolite provides an example of cumulate pyroxenite formation in the Neoproterozoic Arabian-Nubian Shield (Hussein et al., 2004). Pyroxenites occur also as veins and dikes crosscutting ophiolitic upper-mantle peridotites (Varfalvy et al., 1997). The formation of pyroxenite dikes and veins can be attributed to the metasomatism of mantle peridotite by melt or fluid migration derived from the subducted slab (Berly et al., 2006). Another possibility for the formation of pyroxenite dikes and veins is through the intrusion of discrete magmas derived from a highly depleted mantle source (Edward, 1995).

There are different interpretations for the spatial and petrogenetic relationships between pyroxenites and the rest of the ophiolitic rocks in the Fawakhir area. Nasseef et al. (1980) have reported that the pyroxenites of the Fawakhir ophiolite occur as veins and isolated bodies with no clear genetic relationship with the surrounding serpentinized mantle rocks. They have also reported the presence of pyroxenites at the base of the serpentinites separated by a gradational igneous contact. Stern (1981) and El-Gaby et al. (1984) described a gradual contact between the ophiolitic gabbro and the pyroxenite, which overlies the serpentinites. El-Sayed et al. (1999) reported the pyroxenite as dikes and bands crosscutting and underlying the coarse-grained gabbro. They also noticed the occurrence of local gradual contacts between pyroxenites and the coarse-grained gabbros.

Based on our field observations, the pyroxenite bodies are interpreted as irregular, sheared lenses within the serpentinites close to the contacts with the ophiolitic gabbro. These pyroxenites have geochemical characteristics of supra-subduction zone magma rep-

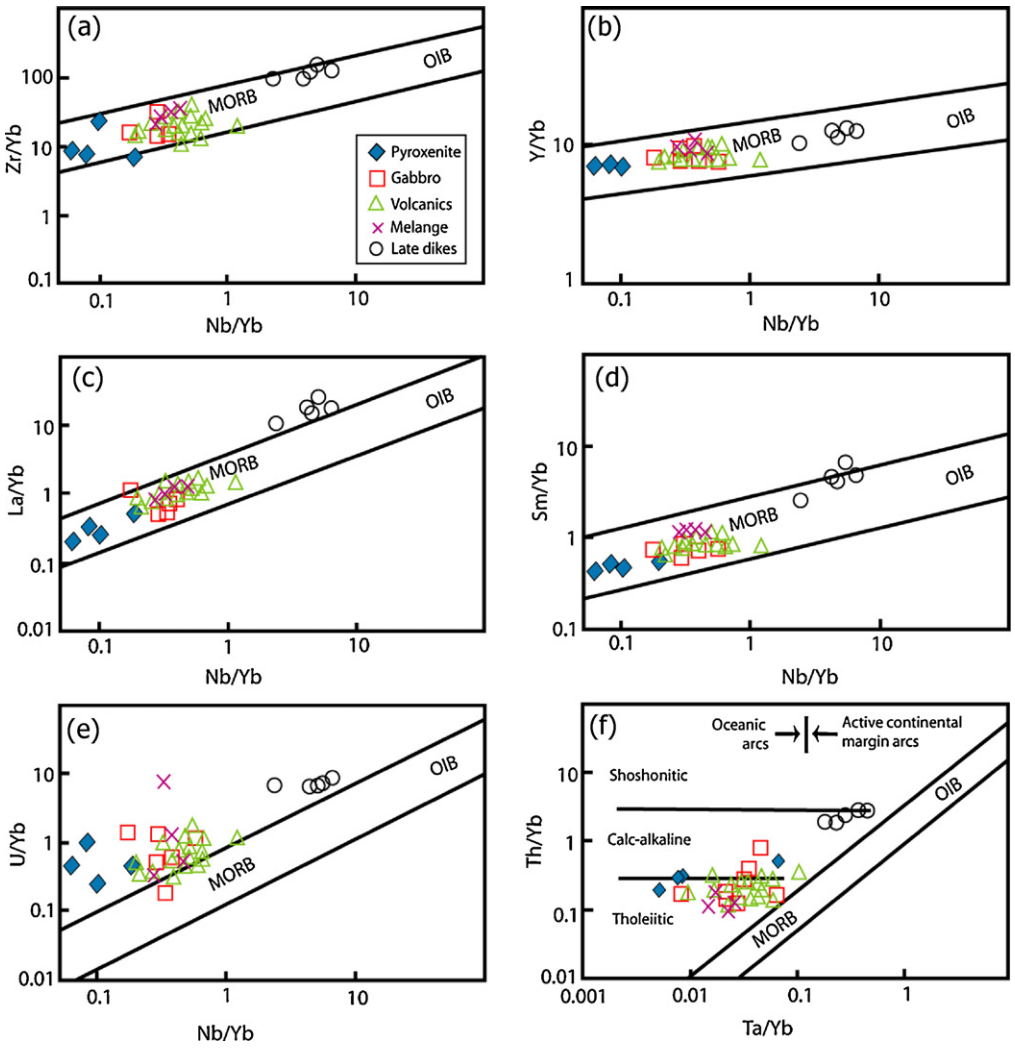

Fig. 12. (a–e) Plot of M/Yb versus Nb/Yb for the ophiolitic rocks and associated dikes at the Wadi Ghadir area where M is (a) Zr, (b) Y, (c) La, (d) Sm, and (e) U. MORB and OIB represent the position of the mid-ocean ridge and oceanic island mantle source respectively. The mantle array (MORB-OIB array) after Green (2006). (f) Th/Yb versus Ta/Yb diagrams with mantle array after Pearce (1983).

resented by enrichment of LILE, LREE and Th and relative depletion of HFSE (Zr, Y) and REE combined with negative Nb anomalies (Hawkins, 2003) (Fig. 8a). On the SiO_2 versus FeO*/MgO diagram, they follow a trend which is different from the one followed by the ophiolitic gabbros and the volcanic rocks (Fig. 9c). These observations imply that the pyroxenites are not a part of cumulates of the Fawakhir ophiolite. Furthermore, as they are enclosed within the serpentinites rather than extend along the contact between the serpentinite and the ophiolitic gabbros, they may represent tectonically disrupted dikes intruding the mantle section such as the pyroxenite dykes recorded by Nasseef et al. (1980) and El-Sayed et al. (1999). The geochemical trend of the pyroxenites on the SiO_2 versus FeO*/MgO diagram (Fig. 9c) is concordant with the boninite-like gabbros identified by El-Sayed et al. (1999). On the TiO_2 versus Al_2O_3/TiO_2 diagram, the pyroxenites and the boninite-like gabbros are extend almost parallel to the other ophiolitic gabbros and volcanic rocks but show lower Ti contents (Fig. 14). Low-Ti trend may indicate re-melting of a highly depleted mantle source (Sun and Nesbitt, 1978). The lower Nb/Yb ratios (Fig. 12) of the pyroxenites support their derivation from a mantle source that is more depleted than the mantle source from which the ophiolitic gabbros and volcanic rocks were derived. The depleted trace element signature of pyroxenites can be acquired by interaction between MORB-like tholeiitic melt and highly depleted mantle or by formation of depleted melt in advanced stage melting of adiabatically upwelling mantle (cf., Kurth-Velz et al., 2004, and references therein). The relatively lower Cr and Ni contents of the pyroxenites minimize the possibility of mantle–melt interaction (cf., Nicolas, 1986). As

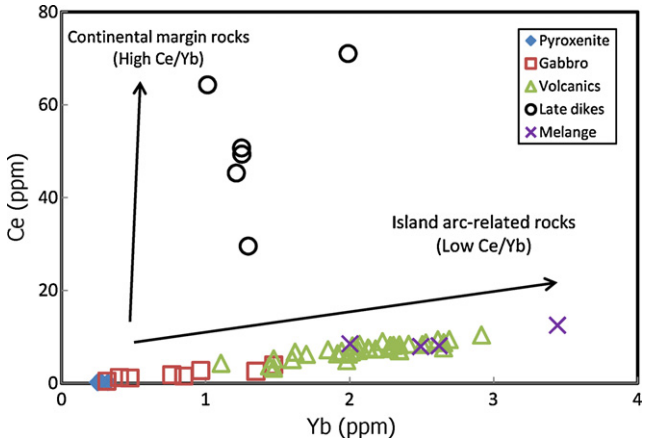

Fig. 13. Variation of Ce and Yb contents of the ophiolitic rocks of the Wadi Ghadir and associated dikes. Island arc (low Ce/Yb) and continental margin (high Ce/Yb) trends are from Hawkesworth et al. (1993).

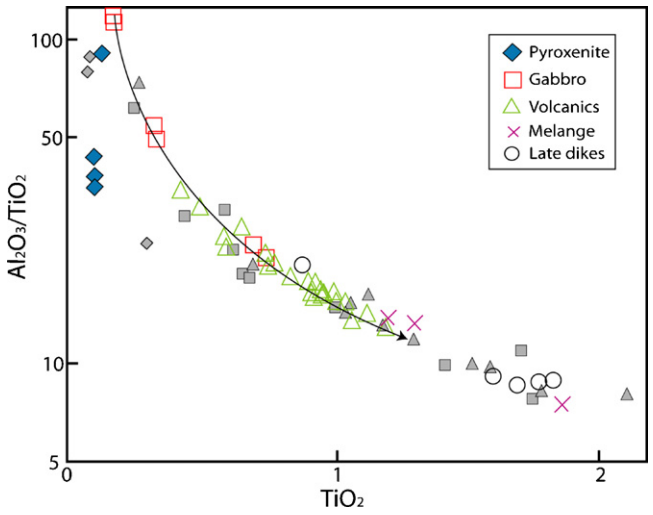

Fig. 14. TiO_2 versus Al_2O_3/TiO_2 diagram. The arrow is visually drawn connecting the Fawakhir ophiolitic gabbros and volcanic rocks. (The grey diamond, square, and triangle symbols are the ophiolitic boninitic gabbro, gabbros, and volcanics respectively from El-Sayed et al., 1999).

inferred by El-Sayed et al. (1999) for the boninite-like gabbros in the Fawakhir ophiolite, the pyroxenites might have originated from poly-baric melting of rising mantle. The uppermost part of the mantle column may have become a highly depleted residue in due course. Melting of this highly depleted mantle might have been facilitated by hydrous input from the subducted slab.

In summary, the Fawakhir pyroxenites are characterized by high MgO and SiO_2 (Table 2). The low Nb/Yb ratios are consistent with their derivation from a highly depleted mantle source. The enrichment of LILE and LREE relative to HFSE and negative Nb anomalies indicate their formation in a supra-subduction zone (Fig. 8a). These pyroxenites show some geochemical similarities to the boninite-like gabbros described by El-Sayed et al. (1999). Both the pyroxenite and the boninite-like gabbros may represent the late-stage magmatic episode in a trench-rollback system, as observed in most Tethyan ophiolites (Dilek et al., 2007, 2008; Dilek and Furnes, 2009; Shervais, 2001).

7.6. Geodynamic setting

Geochemical characteristics of the Fawakhir ophiolite, such as the enrichment of LILE, LREE and Th over HFSE (Zr, Y) in conjunction with negative Nb anomalies on primitive mantle-normalized diagrams, are consistent with its evolution in a supra-subduction zone tectonic setting (cf., Pearce, 2003). Previous workers (i.e., El-Gaby et al., 1984; El-Sayed et al., 1999) have concluded that the Fawakhir ophiolite may represent a supra-subduction oceanic crust that formed in a back-arc environment.

Supra-subduction zone ophiolites have island arcs geochemical affinities but the structure of oceanic crust is formed by seafloor spreading processes (Pearce et al., 1984; Dilek et al., 1998; Dilek et al., 2007; Metcalf and Shervais, 2008). These ophiolites form during the initial stages of subduction, ridge-trench intersection, and back-arc rifting and spreading (Pearce, 2003). Subduction initiation is considered as the most important process for ophiolite formation within the life cycle of a supra-subduction ophiolite (Casey and Dewey, 1984; Shervais, 2001). With subduction initiation, the early, infant arc (or pre-arc as mentioned by Pearce et al., 1984) magmatism is characterized by depleted arc tholeiitic and boninitic magmas that occur in extensional environments similar to slow-spreading centers (Stern and Bloomer, 1992; Bloomer et al., 1995). The formation of many Phanerozoic ophiolites has been attributed

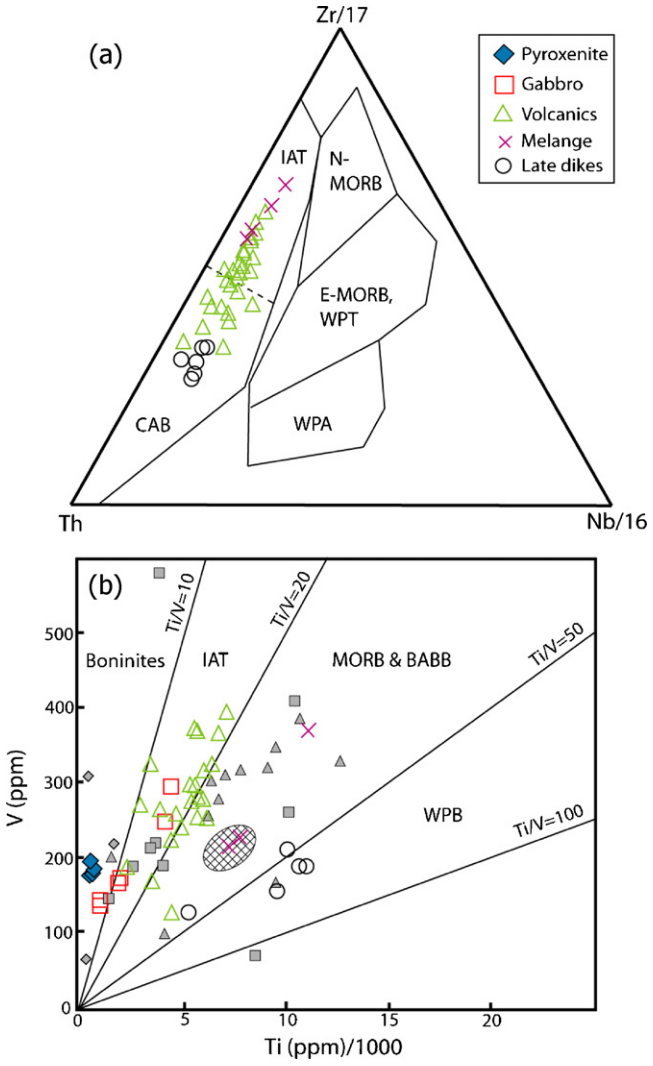

Fig. 15. Tectonic discrimination diagrams of the Fawakhir ophiolite, eastern mélange and late dikes. (a) Th–Zr/17–Nb/16 diagram of Wood (1980). (b) Ti/1000 versus V diagram of Shervais (1982). IAT is island arc tholeiitic, CAB is calc-alkaline basalt, N-MORB is normal mid-ocean ridge basalt, E-MORB is enriched mid-ocean ridge basalt, WPT is within plate tholeiitic, WPA is within plate alkalic, WPB is within plate basalt, BABB is back-arc basin basalt. (The grey diamond, square, and triangle symbols are the ophiolitic boninitic gabbro, gabbros, and volcanics respectively from El-Sayed et al., 1999; the hatched field is the metabaslts from Wadi Ambagui area after El-Mahallawi, 1994.)

to subduction initiation (Casey and Dewey, 1984; Shervais, 2001). The forearc crust of the Izu-Bonin-Mariana (IBM) arc system in the Western Pacific is a good example of infant-arc formation (Stern and Bloomer, 1992; Bloomer et al., 1995).

The Fawakhir ophiolite is composed mainly of low-Ti tholeiitic rocks and has a poorly developed sheeted dike complex. Although rocks of boninitic affinity were not found in our study, they have been reported by El-Sayed et al. (1999). The pyroxenite intrusions within the serpentinized peridotites may also indicate the presence of a highly depleted mantle source (cf., Kurth-Velz et al., 2004). These features collectively suggest that the Fawakhir ophiolite may have formed in an incipient arc–forearc setting during subduction initiation (cf., Stern and Bloomer, 1992).

On the Cr versus Y diagram (Pearce et al., 1984), the Fawakhir ophiolite plots within the arc field, similar to the Mariana forearc crustal rocks (Fig. 10). On other discrimination diagrams, such as Ti–V and Th–Zr–Nb, the gabbros and volcanic rocks also plot in the island arc field (Fig. 15). Pyroxenite and boninitic gabbros from the

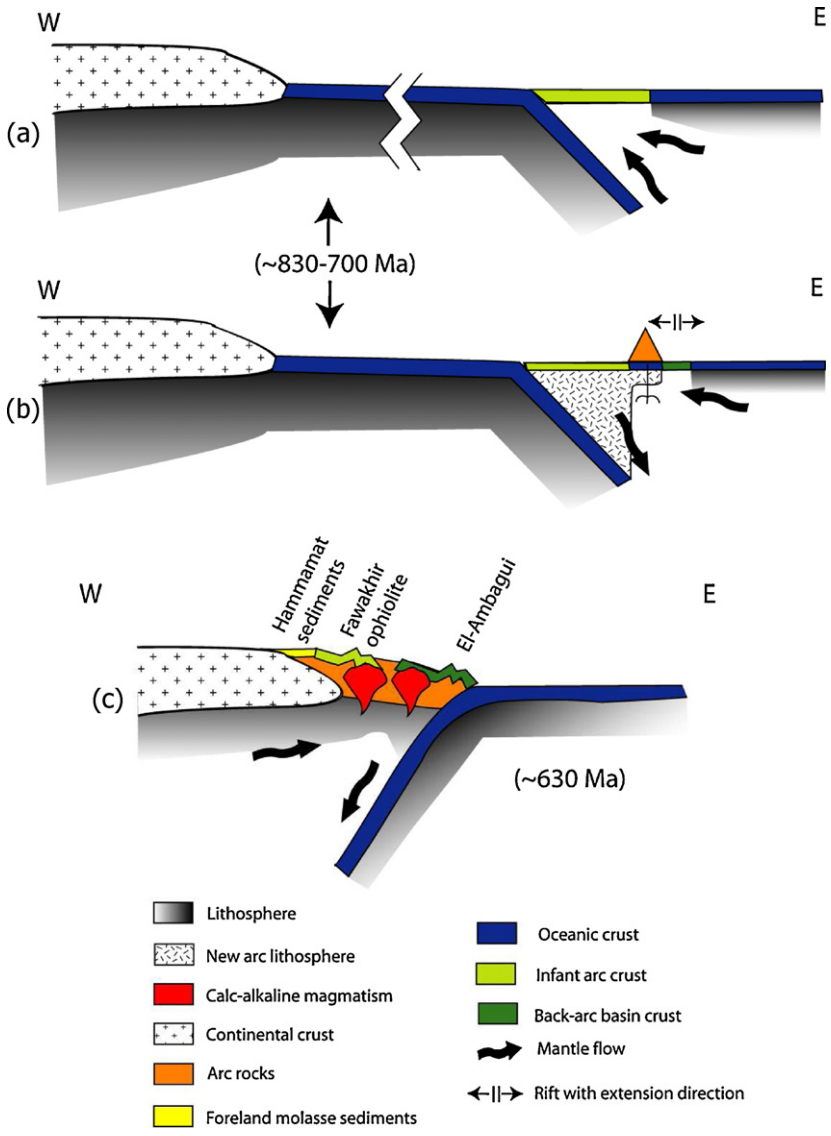

Fig. 16. Schematic model for the history of tectonic evolution of the Fawakhir ophiolite and Central Eastern Desert along the Qift-Qusier Road. (a) The formation of infant arc crust and lithosphere. (b) The formation of arc–back-arc rocks with the cession of forearc extensional stresses and beginning of true subduction. (c) Obduction–accretion of the oceanic crusts and reversing the subduction polarity from east-dipping to west-dipping and the formation of calc-alkaline magmatism related to Andean-type continental margin and associated foreland sedimentation of Hammamat sediment (a and b are depicted from Fig. 8 of Stern and Bloomer, 1992). Orientations are in the present coordinate system and ages are approximate after Stern (2008).

Fawakhir area are also plotted on the Ti–V diagram to compare them with the ophiolitic gabbros and volcanic rocks (Fig. 15b). The pyroxenites extend within the boninitic field of the Ti–V plot along with the boninitic gabbro of El-Sayed et al. (1999). The extended trend of the pyroxenites and the boninitic gabbros in very low Ti/V field suggests derivation of their magmas by low-pressure partial melting of more depleted, relative to the Fawakhir ophiolitic gabbro and volcanic rocks, mantle source that was metasomatized by fluids derived from the subducted slab (cf., Bonev and Stampfli, 2009).

The infant-arc signature and structure of the Fawakhir ophiolite is consistent with the appearance of depleted harzburgite mantle rocks in the Eastern Desert similar to ultramafic rocks from modern forearc tectonic settings (Fig. 16a; Azer and Stern, 2007; Khalil and Azer, 2007). The association of arc tholeiitic gabbros and volcanic rocks, and pyroxenite dykes derived from more refractory source represents the early stages (birth and youth) of an ophiolite life cycle described from the Tethyan ophiolites (Shervais, 2001; Dilek and Furnes, 2009). The birth stage represents the subduction initiation and formation of the Fawakhir oceanic crust and the youth stage represents re-melting of the depleted mantle. These stages are also recorded in other Phanerozoic ophiolites, such as the Troodos (Cyprus), Semail (Oman), Vourinos (Greece), and Betts Cove (Newfoundland) (Bédard et al., 1998; Dilek and Furnes, 2009).

Volcanic blocks within the mélange, to the east of the Fawakhir ophiolite, and closer to the Wadi Ambagui area (Fig. 2), also have a supra-subduction geochemical signature, as they are enriched in Th and LREE relative to HFSE (Nb, Zr, Y) (Fig. 8c). Although both rock assemblages have similar Mg-numbers, the eastern mélange blocks have higher TiO_2 (0.83–1.86 wt%) than the Fawakhir ophiolite (0.15–1.18 wt%). High TiO_2 and a supra-subduction signature can be attributed to formation in a back-arc tectonic setting (cf., Serri, 1981). The higher Al_2O_3/TiO_2 ratios of the Fawakhir volcanic rocks relative to the eastern mélange indicates a transition from an island arc tholeiite (IAT) signature in the west to a MORB-like signature in the east (cf., Sun and Nesbitt, 1978). On the Cr versus Y and Ti versus V tectonic discrimination diagrams, the eastern mélange blocks plot in the MORB field together with the basalts of Wadi Ambagi (Figs. 10 and 15). The IAT and MORB geochemical

association is a feature of rocks formed in a back-arc environment (see Pearce et al., 1984). The transitional characteristic of the pillow lavas of the eastern mélange between MORB and IAT affinities are seen on the Th–Zr–Nb ternary diagram (Fig. 15a). The eastern mélange lavas plot closer to the MORB field than the Fawakhir ophiolitic volcanic rocks. The pillow basalts of the eastern mélange may have been part of the Wadi Ambagi belt, which is interpreted to have formed in a mid-ocean ridge setting (El-Mahallawi, 1994). Given the mobility of LILE and the lack of Nb data in his analyses, it is likely that back-arc basin basalts were interpreted as MORB by El-Mahallawi (1994).

The geochemical similarities between the Fawakhir ophiolite and Izu-Bonin-Mariana forearc crust and between the eastern mélange block and Mariana Trough rocks may indicate the presence of a Neoproterozoic forearc–back-arc association analogous to the Mariana arc system (Fig. 16b). Spatial variation in geochemical signatures from back-arc-like mélange blocks in the east to the forearc Fawakhir ophiolite in the west suggests that the subduction direction was likely to the east (in the present coordinate system). The same approach was used by Khan et al. (1997) to predict the subduction polarity of the Kohistan intra-oceanic arc. Near Marsa Alam, the same east-dipping subduction polarity was inferred for the formation of the Ghadir ophiolite (Abd El-Rahman et al., 2009).

The forearc Fawakhir ophiolite to the west and the back-arc eastern mélange are separated by Meatiq gneissic dome (Fig. 2). The ages of these gneisses are a matter of debate (Andresen et al., 2009, and reference therein). Loizenbauer et al. (2001) interpreted the Meatiq gneissic dome as a metamorphic core complex. The exhumation of the deeper crustal rocks at the Meatiq dome may have caused the erosion of the intervening arc edifice separating the forearc crust to the west and the back-arc rocks to the east. Some exposures of andesitic volcaniclastic rocks were noticed within the mélange to the east of the Meatiq dome, between the Wadi Ambagui and the Meatiq dome. These andesitic volcaniclastic rocks could be part of the arc belt exposed in the Wadi Hammariya area. The Wadi Hammariya extends parallel to the Qift-Qusier Road and is covered mainly by metamorphosed island arc belt that extends to the south of the Meatiq dome (Abdel-Karim et al., 2008). This island arc belt may represent part of the island arc edifice separating the Fawakhir forearc ophiolite from the eastern mélange with back-arc geochemical signature. Ali et al. (2009) reported the extension of the island arc belt and the back-arc assemblage further to the south of Wadi Hammariya.

The Fawakhir ophiolite is intruded by younger evolved calc-alkaline dikes. These post-ophiolitic dikes have lower Mg-number, Cr and Ni contents, have a subduction signature represented by Th and LREE enrichment over HFSE (Nb, Zr, Y), and plot in the calc-alkaline basalt field of the Th–Zr–Nb tectonic discrimination diagram (Figs. 8d and 15a). They are different from the ophiolitic and mélange rocks in that they have higher concentrations of Nb over Zr and Zr over Y, and high Ce/Yb ratios (Fig. 13), which indicate a contribution from a source enriched in incompatible elements such as sub-continental lithospheric mantle (cf., Pearce, 1983). Both the petrography and geochemistry of the calc-alkaline dikes are similar to the Dokhan Volcanic unit of the Eastern Desert (see Basta et al., 1980; Eliwa et al., 2006). Calc-alkaline dikes and the Dokhan volcanic rocks represent Andean-type rocks that were emplaced in an active continental margin (El-Gaby et al., 1988; Abdel Rahman, 1996; Eliwa et al., 2006; Alaabed and El Tokhi, 2009). We infer that the post-ophiolitic calc-alkaline dikes crosscutting the Fawakhir ophiolite were emplaced after the accretion of the intra-oceanic arc–forearc system onto the continental margin and the subsequent reversal of subduction direction to a west-dipping one beneath the Saharan craton (Fig. 16c). Formation of the Andean-type continental margin gave rise to calc-alkaline magmatism derived partly from partial melting of the sub-continental lithospheric mantle in the Eastern Desert at ca. 620–710 Ma (Stern and Hedge, 1985; Loizenbauer et al., 2001; Eliwa et al., 2006). Subsequently, and with the subduction polarity reversal, a Cordilleran stage in the tectonic evolution of the Eastern Desert (reported by El-Gaby et al., 1988) started (Fig. 16c). Production of continental arc magmatism following the island arc accretion and reversal of the subduction polarity has been documented in several ancient orogens such as the Mesoproterozoic Grenville orogen (Martin and Dickins, 2005), the Paleozoic Appalachian–Caledonian orogen (Van Staal et al., 1998), the Mesozoic collision between the Kohistan arc and Karakorum (Khan et al., 1997), and Ecuadorian Western Cordilleran margin (Vallejo et al., 2009), as well as for the Western Pacific island systems such as the Luzon (Clift et al., 2003) and Papua New Guinea arcs (Harris, 2003).

8. Conclusions

In this study, we used high-precision geochemical data from the Fawakhir ophiolite and mélange fragments from Qift-Qusier Road in the Eastern Desert to assess the geodynamic evolution of this part of the Arabian-Nubian Shield. Previously proposed models for the evolution of the Arabian-Nubian Shield assigned a back-arc tectonic setting for the Neoproterozoic oceanic crust in the Eastern Desert (El-Bayoumi, 1983; El-Sayed et al., 1999; Farahat et al., 2004). The trace element geochemical characteristics of the crustal rocks in the Fawakhir ophiolite (La/Sm_{cn} = 2.13–2.48, Gd/Yb_{cn} = 2.04–4.25, Th/Nb_{pm} = 3.2–5.8, La/Nb_{pm} = 2.5–4.9) are consistent with a supra-subduction zone tectonic setting. The Fawakhir ophiolite appears to have originated during the initiation of an intra-oceanic subduction, as in the Izu-Bonin-Mariana forearc system. The Fawakhir magmas were derived from melting of a variably depleted, N-MORB-like, mantle source within the spinel stability field.

A west-dipping subduction interpretation is a widely accepted model to account for the subduction zone geochemical signature of the ophiolitic rocks in the Eastern Desert (El-Bayoumi and Greiling, 1984; Kröner, 1985; Kröner et al., 1987). Although Ries et al. (1983) proposed an east-dipping subduction direction; their model could not account for supra-subduction signatures of the Neoproterozoic ophiolites in the region (see Kröner et al., 1987). In this study and on the basis of spatial variation of the geochemical data along the Qift-Qusier Road (Fig. 2), we propose that subduction direction reversed from east to west following the accretion of the Fawakhir ophiolite onto the West Gondwana margin (Saharan craton) at about 630 Ma (Fig. 16). The mélange blocks to the east of the Fawakhir ophiolite are compositionally similar to present-day back-arc basin volcanic rocks, whereas volcanic rocks of the Fawakhir ophiolite have a forearc geochemical signature (Fig. 10). Accordingly, the compositional difference and spatial relationships between the western Fawakhir ophiolite and the eastern mélange blocks are consistent with an east-dipping subduction direction during the formation of these rocks in an intra-oceanic arc system.

Following the accretion of the incipient arc–forearc units onto the western Gondwana margin, the Fawakhir ophiolitic rocks were intruded by basaltic to andesitic calc-alkaline dikes. The geochemical data for the post-ophiolitic calc-alkaline dikes (Ce/Yb = 23–63, Zr/Yb = 101–160) are consistent with the formation of their magmas at an Andean-type continental margin. These dykes are undeformed and exhibit lower degrees of metamorphism. The systematic enrichment of their magmas in highly immobile incompatible elements, similar to other calc-alkaline rocks formed in active continental margins, indicates contributions from an enriched source such as sub-continental lithospheric mantle (cf., Pearce, 1983). One of the reasons stated by Kröner et al. (1987) to refute the east-dipping subduction model of Ries et al. (1983) is the difficulty in generating calc-alkaline magmatism, characteriz-

ing the Cordilleran stage of the evolution of the Eastern Desert, from a mantle below a passive continental margin of West Gondwana.

Acknowledgements

Two reviewers (anonymous and J. Dostal) and editor (P. Cawood) are acknowledged for their constructive comments, which have resulted in significant improvements to the paper. We thank J.C. Barrette, J.C. Ordóñez-Calderón and Zhaoping Yang for their help during geochemical analyses. This is a contribution of PREA and NSERC grants (250926) to A. Polat and NSERC grant (83117) to B. Fryer.

Appendix A. Supplementary data

Supplementary data associated with this article can be found, in the online version, at doi:10.1016/j.precamres.2009.09.008.

References

Abd El-Naby, H., Frisch, W., 2006. Geochemical constraints from the Hafafit Metamorphic Complex (HMC): evidence of Neoproterozoic back-arc basin development in the central Eastern Desert of Egypt. Journal of African Earth Sciences 45, 173–186.

Abd El-Rahman, Y., Polat, A., Dilek, Y., Fryer, B.J., El-Sharkawy, M., Sakran, S., 2009. Geochemistry and tectonic evolution of the Neoproterozoic Wadi Ghadir ophiolite, Eastern Desert, Egypt. Lithos, doi:10.1016/j.lithos.2008.12.014.

Abdel-Karim, A.M., Azzaz, S.A., Moharem, A.F., El-Alfy, H.M., 2008. Petrological and geochemical studies on the ophiolite and island arc association of Wadi Hammariya, Central Eastern Desert, Egypt. The Arabian Journal for Science and Engineering 33, 117–138.

Abdel Rahman, A.M., 1996. Pan-African volcanism: petrology and geochemistry of the Dokhan Volcanic suite in the northern Nubian Shield. Geological Magazine 133, 17–31.

Ahmed, A.H., Arai, S., Attaia, A.K., 2001. Petrological characteristics of the Pan African podiform chromatite and associated peridotites of the Proterozoic ophiolite complexes, Egypt. Mineralium Deposita 36, 72–84.

Alaabed, S., El Tokhi, M., 2009. Petrogenesis of Pan-African Dokhan Volcanics of the Northeastern Desert, Egypt: mineralogy and geochemistry consideration. Goldschmidt Conference Abstract 2009, A20.

Ali, K.A., Stern, R.J., Manton, W.I., Kimura, J.-I., Khamis, H.A., 2009. Geochemistry Nd isotopes and U–Pb SHRIMP zircon dating of Neoproterozoic volcanic rocks from the Central Eastern Desert of Egypt: New insight into the ~750 Ma crust-forming event. Precambrian Research 171, 1–22.

Andresen, A., Abu El-Rus, M.A., Myhre, P.I., Boghdady, G.Y., Corfu, F., 2009. U–Pb TIMS age constraints on the evolution of the Neoproterozoic Meatiq Gneiss Dome, Eastern Desert, Egypt. International Journal of Earth Sciences 98, 481–497.

Arculus, R.J., 2003. Use and abuse of the terms calc-alkaline and calc-alkalic. Journal of Petrology 44, 929–935.

Azer, M.K., Stern, R.J., 2007. Neoproterozoic (835–720 Ma) serpentinites in the Eastern Desert, Egypt: fragments of forearc mantle. The Journal of Geology 115, 457–472.

Barrett, T.J., MacLean, W.H., 1994. Chemostratigraphy and hydrothermal alteration in exploration for VHMS deposits in greenstone and younger volcanic rocks. In: Lentz, D.R. (Ed.), Alteration and Alteration Processes Associated with Ore-Forming Systems. Geological Association of Canada, Short Course Notes 11, pp. 433–467.

Basta, E.Z., Kotb, H., Awadalla, M.F., 1980. Petrochemical and chemical characteristics of the Dokhan formation at the type locality, Gebel Dokhan, Eastern Desert, Egypt. Bulletin of King Abdelaziz University 3, 121–140.

Bédard, J.H., Lauziere, K., Tremblay, A., Sangster, A., 1998. Evidence for forearc seafloor spreading from the Betts Cove ophiolite, Newfoundland: oceanic crust of boninitic affinity. Tectonophysics 284, 233–245.

Berly, T.J., Hermann, J., Arculus, R.J., Lapierre, H., 2006. Supra-subduction zone pyroxenites from San Jore and Santa Isabel (Solomon Isalnds). Journal of Petrology 47, 1531–1555.

Bloomer, S.H., Taylor, B., MacLeod, C.J., Stern, R.J., Fryer, P., Hawkins, J.W., Johnson, L., 1995. Early arc volcanism and the ophiolite problem: a perspective from drilling in the Western Pacific. In: Taylor, B., Natland, J. (Eds.), Active Margins and Marginal Basins of the Western Pacific. AGU Geophysical Monograph 88, pp. 1–30.

Bonev, N., Stampfli, G., 2009. Gabbro, plagiogranite, and associated dikes in the suprasubduction zone Evros Ophiolite, NE Greece. Geological Magazine 146, 72–91.

Casey, J.F., Dewey, J.F., 1984. Initiation of subduction zone along transform and accreting plate boundaries, triple-junction evolution, and forearc spreading centers; implications for ophiolitic geology and obduction. In: Gass, I.G., Lippard, S.J., Shelton, A.W. (Eds.), Ophiolites and Oceanic Lithosphere. Geological Society, London, Special Publication 13, pp. 269–290.

Clift, P.D., Schouten, H., Draut, A.E., 2003. A general model of arc-continent collision and subduction polarity reversal from Taiwan and Irish Caledonides. In: Larter, R.D., Leat, E.T. (Eds.), Intra-oceanic Subduction Systems: Tectonic and Magmatic Processes. Geological Society, London, Special Publication 219, pp. 81–98.

Davidson, J.P., 1996. Deciphering mantle and crystal signatures in subduction zone magmatism. Subduction: top to bottom. Geophysical Monograph 96, AGU, Washington, pp. 251–262.

Dilek, Y., Ahmed, Z., 2003. Proterozoic ophiolites of the Arabian Shield and their significance in Precambrian tectonics. In: Dilek, Y., Robinson, P.T. (Eds.), Ophiolite in Earth History. Geological Society, London, Special Publication 218, pp. 685–700.

Dilek, Y., Moores, E.M., Furnes, H., 1998. Structure of modern oceanic crust and ophiolites and implications for faulting and magmatism at oceanic spreading centers. In: Buck, R., Karson, J., Delaney, P., Lagabrielle, Y. (Eds.), AGU Monograph on Faulting and Magmatism at Mid-Ocean Ridges, 106, pp. 219–266.

Dilek, Y., Furnes, H., Shallo, M., 2007. Suprasubduction zone ophiolite formation along the periphery of Mesozoic Gondwana. Gondwana Research 11, 453–475.

Dilek, Y., Furnes, H., Shallo, M., 2008. Geochemistry of the Jurassic Mirdita ophiolite (Albania) and the MORB to SSZ evolution of a marginal basin oceanic crust. Lithos 100, 174–209.

Dilek, Y., Furnes, H., 2009. Structure and geochemistry of Tethyan ophiolites and their petrogenesis in subduction rollback systems. Lithos, doi:10.1016/j.lithos.2009.04.022.

Edward, S.J., 1995. Boninitic and tholeiitic dykes in the Lewis Hills mantle section of the Bay of Islands ophiolite: implications for magmatism adjacent to a fracture zone in a back-arc spreading environment. Canadian Journal of Earth Sciences 32, 2128–2146.

El-Bayoumi, R.M., 1983. Ophiolites and mélange complex of Wadi Ghadir area, Eastern Desert, Egypt. Bulletin of King Abdelaziz University 6, 329–342.

El-Bayoumi, R.M.A., Greiling, R.O., 1984. Tectonic evolution of a Pan-African plate margin in southeastern Egypt—a suture zone overprinted by low angle thrusting? In: Klerkx, J., Michot, J. (Eds.), Géologie Africaine-African Geology. Musee royal de l'Africaine Centrale, Tervuren, Belg, pp. 47–56.

El-Gaby, S., El-Nady, O., Khudeir, A., 1984. Tectonic evolution of the basement complex in the Central Eastern Desert of Egypt. Geologische Rundschau 73, 1019–1036.

El-Gaby, S., List, F.K., Tehrani, R., 1988. Geology, evolution and metallogenesis of the Pan-African belt in Egypt. In: El-Gaby, S., Greiling, R.O. (Eds.), The Pan-African Belt of Northeast Africa and Adjacent Areas: Tectonic Evolution and Economic Aspects of a Late Proterozoic Orogen, Friedrich. Vieweg, Sohn Verlagsgesellschaft mbH, pp. 17–68.

El-Mahallawi, M.M., 1994. Contribution to the geochemistry and petrogenesis of some metabasalts from the Ambagi Area, Central Eastern Desert, Egypt. Egyptian Journal of Geology 38, 401–419.

El-Shafei, M.K., Kusky, T.M., 2003. Structural evolution of the Neoproterozoic Feiran-Solaf metamorphic belt, Senai Peninsula: implications for the closure of the Mozambique Ocean. Precambrian Research 126, 269–293.

El-Sayed, M.M., Furnes, H., Mohamed, F.H., 1999. Geochemical constraints on the tectonomagmatic evolution of the late Precambrian Fawakhir ophiolite, Central Eastern Desert, Egypt. Journal of African Earth Science 29, 515–533.

Eliwa, H.A., Kimura, J.I., Itaya, T., 2006. Late Neoproterozoic Dokhan volcanic rocks, northern Eastern Desert, Egypt. Precambrian Research 151, 31–52.

Farahat, E.S., 2008. Chrome-spinels in serpentinites and talc carbonates of the El Edeid-El Sodmein District, Central Eastern Desert, Egypt: their metamorphism and petrogenetic implication. Chemie de Erde Geochemistry 68, 193–205.

Farahat, E.S., El Mahalawi, M.M., Hoinkes, G., Abdel Aal, A.Y., 2004. Continental back-arc basin origin of some ophiolites from the Eastern Desert of Egypt. Mineralogy and Petrology 82, 81–104.

Fowler, T.J., Osman, A.F., 2001. Gneiss-cored interference dome associated with two phases of late Pan-African thrusting in the Central Eastern Desert, Egypt. Precambrian Research 108, 17–43.

Furnes, H., El-Sayed, M.M., Khalil, S.O., Hassanen, M.A., 1996. Pan-African magmatism in the Wadi El-Imra District, central Eastern Desert, Egypt; geochemistry and tectonic environment. Journal of Geological Society of London 153, 705–718.

Furnes, H., Skjerlie, K.P., Dilek, Y., 2000. Petrology, tectonics, and hydrothermal alteration of a back-arc oceanic crust: Solund-Stavfjord ophiolite complex of the western Norwegian Caledonides: a review. In: Dilek, Y., Robinson, P.T. (Eds.), Ophiolites and Oceanic Crust; New Insights from Field Studies and the Ocean Drilling Program. GSA Spec. Paper 349, pp. 443–460.

Gardien, V., Lecuyer, C., Moyen, J.-F., 2008. Dolerites of the Woodlark basin (Papuan Peninsula, New Guinea): a geochemical record on the influence of a neighboring subduction zone. Journal of Asian Earth Sciences 33, 139–154.

Gillis, K.M., Banerjee, N.R., 2000. Hydrothermal alteration patterns in supra-subduction zone ophiolites. In: Dilek, Y., Moores, E.M., Elthon, D., Nicolas, A. (Eds.), Ophiolites and Oceanic Crust: New Insights from Field Studies and the Ocean Drilling Program. Geological Society of America Special Paper 349, 283–297.

Green, N.L., 2006. Influence of slab thermal structure on basalt source regions and melting conditions: REE and HFSE constraints from the Garibaldi volcanic belt, northern Cascadia subduction system. Lithos 87, 23–49.

Greiling, R.O., Abdeen, M.M., Dardir, A.A., El Akhal, H., El Ramly, M.F., Kamal El Din, G.M., Osman, A.F., Rashwan, A.A., Rice, A.H.N., Sadek, M.F., 1994. A structural synthesis of the Proterozoic Arabian-Nubian Shield in Egypt. Geologie Rundschau 83, 484–501.

Harris, R., 2003. Geodynamic patterns of ophiolites and marginal basins in the Indonesian and New Guinea regions. In: Dilek, Y., Robinson, P.T. (Eds.), Ophi-

olite in Earth History. Geological Society, London, Special Publication 218, pp. 481–506.
Hawkesworth, C.J., Gallagher, K., Hergt, J.M., McDermott, F., 1993. Mantle and slab contributions in arc magmas. Annual Review of Earth and Planetary Sciences 21, 175–204.
Hawkins, J.W., 2003. Geology of supra-subduction zones—implications for the origin of ophiolites. In: Dilek, Y., Newcomb, S. (Eds.), Ophiolite Concept and the Evolution of Geological Thought. Boulder, CO, Geological Society of America Special Paper 373, pp. 227–268.
Hirschmann, M.M., Stolper, E.M., 1996. A possible role for garnet pyroxenite in the origin of the "garnet signature" in MORB. Contribution Mineralogy and Petrology 124, 185–208.
Hofmann, A.W., 1988. Chemical differentiation of the Earth: the relationship between mantle continental crust and oceanic crust. Earth and Planetary Science Letters 90, 297–414.
Humphries, S.E., 1984. The mobility of the rare earth elements in the crust. In: Henderson, P. (Ed.), Rare Earth Element Geochemistry. Elsevier, Amsterdam, pp. 317–342.
Hussein, I.M., Kröner, A., Reischmann, T., 2004. The Wadi Onib mafic–ultramafic complex: a Neoproterozoic supra-subduction zone ophiolite in the northern Red Sea Hills of the Sudan. In: Kusky, T.M. (Ed.), Precambrian Ophiolites and Related Rocks. Developments in Precambrian Geology, vol. 13. Elsevier, Amsterdam, pp. 163–206.
Jenner, G.A., Longerich, H.P., Jackson, S.E., Freyer, B.J., 1990. ICP-MS—a powerful tool for high-precision trace-element analysis in earth sciences: evidence from analysis of selected U.S.G.S. reference samples. Chemical Geology 83, 133–148.
John, T., Klemd, R., Gao, J., Garbe-schönberg, C.-D., 2008. Trace-elements mobilization in slabs due to nonsteady-state fluid-rock interaction: constraints from an eclogite-facies transform vein in blueschist (Tianshan, China). Lithos 103, 1–24.
Jöns, N., Schenk, V., 2007. Relics of the Mozambique Ocean in the central Eastern African Orogen: evidence from the Vohibory Block of southern Madagascar. Journal of Metamorphic Geology 26, 17–28.
Kessel, R., Schmidt, M.W., Ulmer, P., Pettke, T., 2005. Trace element signature of subduction-zone fluids, melts and supercritical fluids at 120–180 km depths. Nature 437/29, 724–727.
Khalil, A.E.S., Azer, M.K., 2007. Supra-subduction affinity in the Neoproterozoic serpentinites in the Eastern Desert, Egypt: evidence from mineral composition. Journal of African Earth Sciences 49, 136–152.
Khalil, K.I., 2007. Chromite mineralization in ultramafic rocks of the Wadi Ghadir area, Eastern Desert, Egypt: mineralogical, microchemical and genetic study. Neues Jahrbuch für Mineralogie: Abhandlungen 183, 283–296.
Khan, M.A., Stern, R.J., Gribble, R.F., Windley, B.F., 1997. Geochemical and isotopic constraints on subduction polarity, magma sources, and paleogeography of the Kohistan intra-oceanic arc, northern Pakistan Himalaya. Journal of Geological Society 154, 935–946.
Kröner, A., 1985. Ophiolites and the evolution of tectonic boundaries in the late Proterozoic Arabian-Nubian Shield of northeast Africa and Arabia. Precambrian Research 27, 277–300.
Kröner, A., Greiling, R.O., Reischmann, T., Hussein, I.M., Stern, R.J., Durr, S., Kruger, J., Zimmer, M., 1987. Pan-African crustal evolution in the Nubian segment of northeast Africa. In: Kröner, A. (Ed.), Proterozoic lithospheric evolution. American Geophysical Union, Geodynamics Series 17, pp. 237–257.
Kröner, A., Todt, W., Hussein, I.M., Mansour, M., Rashwan, A.A., 1992. Dating of late Proterozoic ophiolites in Egypt and the Sudan using the single grain zircon evaporation technique. Precambrian Research 59, 15–32.
Kurth-Velz, M., Sassen, A., Galer, S.J.G., 2004. Geochemical and isotopic heterogeneities along and island arc-spreading ridge intersection: evidence from the Lewis Hills, Bay of Isalnds ophiolite, Newfoundland. Journal of Petrology 45, 635–668.
Loizenbauer, J., Wallbrecher, E., Fritz, H., Neumayr, P., Khudier, A.A., Kloetzli, U., 2001. Structural geology, single zircon age and fluid inclusion studies of Meatiq metamorphic core complex: Implication for Neoproterozoic tectonics in the Eastern Desert of Egypt. Precambrian Research 110, 357–383.
Macdonald, R., Hawkesworth, C.J., Heather, E., 2000. The Lesser Antiles volcanic chain: a study in arc magmatism. Earth Science Review 49, 1–76.
Magganas, A.C., 2002. Constraints on the petrogenesis of Evros ophiolite extrusives, NE Greece. Lithos 65, 165–184.
Martin, C., Dickins, A.P., 2005. Styles of Proterozoic crustal growth on the southeast margin of Laurentia: evidence from central Granville Province northwest of Lac St.-Jean, Quebec. Canadian Journal of Earth Science 42, 1643–1652.
Metcalf, R.V., Shervais, J.W., 2008. Suprasubduction zone ophiolites: is there really an ophiolite conundrum? In: Wright, J.E., Shervais, J.W. (Eds.), Ophiolites, Arcs, and Batholiths: A Tribute to Cliff Hopson. GSA Special Paper 438, pp. 191–222.
Miyashiro, A., 1974. Volcanic rock series in island arcs and active continental margins. American Journal of Sciences 274, 321–355.
Nasseef, A.O., Bakor, A.R., Hashad, A.H., 1980. Petrography of possible ophiolitic rocks along the Qift-Qusier Road, Eastern Desert, Egypt. Bulletin of King Abdelaziz University 3, 157–168.
Nicolas, A., 1986. A melt extraction model based on structural studies of mantle peridotites. Journal of Petrology 27, 999–1022.
Ordóñez-Calderón, J.C., Polat, A., Fryer, B., Gagnon, J.E., Raith, J.G., Appel, P.W.U., 2008. Evidence for HFSE and REE mobility during calc-silicate metasomatism, Mesoarchean (~3075 Ma) Ivisaartoq greenstone belt, Southern west Greenland. Precambrian Research 161, 317–340.
Pearce, J.A., 1982. Trace element characteristics of lavas from destructive plate boundaries. In: Thorpe, R.S. (Ed.), Andesites: Orogenic Andesites and Related Rocks. John Wiley, Chichester, pp. 525–547.
Pearce, J.A., 1983. Role of sub-continental lithosphere in magma genesis at active continental margins. In: Hawkesworth, C.J., Norry, M.J. (Eds.), Continental Basalts and Mantle Xenoliths. Shiva, Nantwich, UK, pp. 230–249.
Pearce, J.A., 2003. Supra-subduction zone ophiolites: the search for modern analogues. In: Dilek, Y., Newcomb, S. (Eds.), Ophiolite Concept and the Evolution of Geological Thought. Geological Society of America Special Paper 373, pp. 269–295.
Pearce, J.A., 2008. Geochemical fingerprinting of oceanic basalts with applications to ophiolite classification and the search for Archean oceanic crust. Lithos 100, 14–48.
Pearce, J.A., Baker, P.E., Harvey, P.K., Luff, I.W., 1995. Geochemical evidence for subduction fluxes, mantle melting and fractional crystallization beneath the South Sandwich island arc. Journal of Petrology 36, 1073–1109.
Pearce, J.A., Lippard, S.J., Roberts, S., 1984. Characteristics and tectonic significance of supra-subduction zone ophiolites. In: Kokelaar, P.B., Howells, M.F. (Eds.), Marginal Basin Geology. Geological Society, London, Special Publication 16, pp. 77–94.
Pearce, J.A., Norry, M.J., 1979. Petrogenetic implications of Ti, Zr, Y, and Nb variations in volcanic rocks. Contributions to Mineralogy and Petrology 69, 33–47.
Pearce, J.A., Peate, D.W., 1995. Tectonic implications of the composition of volcanic arc lavas. Annual Review of Earth and Planetary Sciences 23, 251–285.
Polat, A., Hofmann, A.W., 2003. Alteration and geochemical patterns in the 3.7–3.8 Ga Isua greenstone belt, West Greenland. Precambrian Research 126, 197–218.
Ragland, P.C., 1989. Basic Analytical Petrology. Oxford University Press, New York.
Ries, A.C., Shackleton, R.M., Graham, R.H., Fitches, W.R., 1983. Pan-African structures, ophiolites and mélanges in the Eastern Desert of Egypt: a traverse at 26°N. Journal of Geological Society 140, 75–95.
Rollinson, H.R., 1993. Using Geochemical Data: Evaluation, Presentation and Interpretation. Longman/Wyllie, Harlow/New York.
Saunders, A.D., Norry, M.J., Tarney, J., 1991. Fluid influence on the trace element compositions of the subduction zone magmas. Royal Society of London Philosophical Transactions 335, 377–392.
Serri, G., 1981. The petrochemistry of ophiolite gabbroic complexes: a key for the classification of ophiolites into low-Ti and high-Ti types. Earth and Planetary Science Letters 52, 203–212.
Shackleton, R.M., Ries, A.C., Graham, R.H., Fitches, W.R., 1980. Late Precambrian ophiolite mélange in the eastern desert of Egypt. Nature 285, 472–474.
Shervais, J.W., 1982. Ti–V plots and petrogenesis of modern and ophiolitic lavas. Earth and Planetary Science Letters 59, 101–118.
Shervais, J.W., 2001. Birth, death, and resurrection: the life cycle of suprasubduction zone ophiolites. Geochemistry, Geophysics, Geosciences 2, 1010, doi:10.1029/2000GC000080.
Smith, I.E.M., Worthington, T.J., Price, R.C., Gamble, J.A., 1997. Primitive magmas in arc-type volcanic association: example from the southwest Pacific. The Canadian Mineralogist 35, 257–273.
Stern, R.J., 1981. Petrogenesis and tectonic setting of Late Precambrian ensimatic volcanic rocks, Central Eastern Desert of Egypt. Precambrian Research 16, 195–230.
Stern, R.J., 1994. Arc assembly and continental collision in the Neoproterozoic East African Orogen: implications for the consolidation of Gondwanaland. Annual Review of Earth and Planet Sciences 22, 319–351.
Stern, R.J., 2005. Evidence from ophiolites, blueschists, and ultrahigh-pressure metamorphic terranes that modern episodes of subduction tectonics began in Neoproterozoic time. Geology 33, 557–560.
Stern, R.J., 2008. Neoproterozoic crustal growth: the solid Earth system during a critical episode of Earth history. Gondwana Research 14, 33–50.
Stern, R.J., Bloomer, S.H., 1992. Subduction zone infancy: examples from the Eocene Izu-Bonin-Mariana and Jurassic California arcs. Geological Society of American Bulletin 104, 1621–1636.
Stern, R.J., Hedge, C.E., 1985. Geochronologic and isotropic constraints n Late Precambrian crustal evolution in the Eastern Desert of Egypt. American Journal of Science 285, 97–127.
Stern, R.J., Johanson, P.R., Kroner, A., Yibas, B., 2004. Neoproterozoic ophiolites of the Arabian-Nubian Shield. In: Kusky, T.M. (Ed.), Precambrian Ophiolites and Related Rocks. Developments in Precambrian Geology, vol. 13. Elsevier, Amsterdam, pp. 95–128.
Sun, S.-S., McDonough, W.F., 1989. Chemical and systematic of oceanic basalts: implications for mantle composition and processes. In: Saunders, A.D., Norry, M.J. (Eds.), Magmatism in Ocean Basins. Geological Society, London, Special Publication 42, pp. 313–345.
Sun, S.-S., Nesbitt, R.W., 1978. Geochemical irregularities and genetic significance of ophiolitic basalts. Geology 6, 689–693.
Tatsumi, Y., Eggins, S., 1995. Subduction Zone Magmatism. Blackwell Science Inc., Cambridge, MA.
Tatsumi, Y., Kogiso, T., 2003. The subduction factory: its role in the evolution of the Earth's crust and mantle. In: Larter, R.D., Leat, E.T. (Eds.), Intra-oceanic Subduction Systems: Tectonic and Magmatic Processes. Geological Society, London, Special Publication 219, pp. 55–80.
Vallejo, C., Winkler, W., Spikings, R.A., Luzieux, L., Heller, F., Bussy, F., 2009. Mode and timing of terrane accretion in the forearc of the Andes in Ecuador. In: Kay, S.M., Ramos, V.A., Dickinson, W.R. (Eds.), Backbone of the Americas: Shallow Subduction, Plateau Uplift, and Ridge and Terrane Collision: Geological Society of America Memoir, vol. 204, pp. 197–216.

Van Staal, C.R., Dewey, J.F., Mac Niocaill, C., Mckerrow, W.S., 1998. The Cambrian-Silurian tectonic evolution of the northern Appalachians and British Caledonides: history of a complex, west and southwest Pacific-type segment of Iapetus. In: Blundell, D.J., Scott, A.C. (Eds.), Lyell: The Past is the Key to the Present. Geological Society, London, Special Publications 143, pp. 199–242.

Varfalvy, V., Hébert, R., Bédard, J.H., Lafléche, M.R., 1997. Petrology and geochemistry of pyroxenite dykes in upper mantle peridotites of the North Arm Mountain Massif, Bay of Islands ophiolite, Newoundland: implications for the genesis of boninitic and related magmas. The Canadian Mineralogist 35, 543–570.

Winchester, J.A., Floyd, P.A., 1977. Geochemical discrimination of different magma series and their differentiation products using immobile elements. Chemical Geology 20, 325–343.

Wood, D.A., 1980. The application of a Th–Hf–Ta diagram to problems of tectono-magmatic classification and establishing the nature of crustal contamination of basaltic lavas of the British Tertiary volcanic province. Earth and Planetary Science Letters 50, 11–30.

Zanetti, A., D'Antonio, M., Vannucci, R., Raffone, N., Spadea, P., 2009. Fore-arc mantle peridotites and back-arc basin basalts from Izu-Bonin-Mariana subduction factory (ODP LEGs 125 and 195): a modern analog for Mediterranean ophiolites. Geophysical Research Abstracts 11, EGU2009-12859.

Zimmer, M., Kröner, A., Jochum, K.P., Reischmann, T., Todt, W., 1995. The Gabal Gerf complex: a Precambrian N-MORB ophiolite in the Nubian Shield, NE Africa. Chemical Geology 123, 29–51.